AD-A048 315 SRI INTERNATIONAL MENLO PARK CA MOLECULAR PHYSICS CENTER F/G 4/1
PHOTON INTERACTIONS WITH ATMOSPHERIC NEGATIVE IONS.(U)
NOV 77 J T MOSELEY, P C COSBY, J R PETERSON DAAG29-76-C-0023
UNCLASSIFIED SRI-MP-77-114 ARO-13916.2-P NL

END
DATE FILMED
2-78
DDC

ARO 13916.2-P

12

B.S

November 30, 1977

Final Report

PHOTON INTERACTIONS WITH ATMOSPHERIC NEGATIVE IONS

By: J. T. Moseley, P. C. Cosby, and J. R. Peterson

U.S. ARMY RESEARCH OFFICE

Contract DAAG29-76-C-0023
SRI Project PYU-5067

Molecular Physics Center
SRI International
Menlo Park, California 94025

MP 77-114

SECURITY CLASSIFICATION OF THIS PAGE *(When Data Entered)*

REPORT DOCUMENTATION PAGE

READ INSTRUCTIONS BEFORE COMPLETING FORM

1. REPORT NUMBER
2. GOVT ACCESSION NO.
3. RECIPIENT'S CATALOG NUMBER

4. TITLE *(and Subtitle)*

Photon Interactions with Atmospheric Negative Ions,

5. TYPE OF REPORT & PERIOD COVERED

Final Report, 1 April 1976-30 Sept 1977,

6. PERFORMING ORG. REPORT NUMBER

SRI-MP-77-114

7. AUTHOR(s)

J. T. Moseley, P. C. Cosby and J. R. Peterson

8. CONTRACT OR GRANT NUMBER(s)

DAAG29-76-C-0023

9. PERFORMING ORGANIZATION NAME AND ADDRESS

SRI International
333 Ravenswood Avenue
Menlo Park, California 94025

10. PROGRAM ELEMENT, PROJECT, TASK AREA & WORK UNIT NUMBERS

80 p.

11. CONTROLLING OFFICE NAME AND ADDRESS

U.S. Army Research Office
Post Office Box 12211
Research Triangle Park, N.C. 27709

12. REPORT DATE

30 Nov 1977

13. NUMBER OF PAGES

14. MONITORING AGENCY NAME & ADDRESS *(if different from Controlling Office)*

ARO 13916.2-P

15. SECURITY CLASS. *(of this report)*

Unclassified

15a. DECLASSIFICATION/DOWNGRADING SCHEDULE

16. DISTRIBUTION STATEMENT *(of this Report)*

Approved for public release; distribution unlimited.

17. DISTRIBUTION STATEMENT *(of the abstract entered in Block 20, if different from Report)*

18. SUPPLEMENTARY NOTES

The findings in this report are not to be construed as an official Department of the Army position, unless so designated by other authorized documents.

19. KEY WORDS *(Continue on reverse side if necessary and identify by block number)*

photodetachment, photodissociation, negative ions, atmospheric ions, cluster ions, drift tube mass spectrometer

20. ABSTRACT *(Continue on reverse side if necessary and identify by block number)*

Photodestruction cross sections have been measured for seventeen negative ions of atmospheric importance over the wavelength range from 5000 to 8400 Å using a drift tube mass spectrometer coupled with a tunable dye laser. The cross sections vary from zero to nearly 10^{-17} cm^2, and thresholds are found for all ions except O_2^- which are photoactive. Vibrational, electronic and isomeric excited states are observed.

10 to the -17th power sq cms,

DD FORM 1 JAN 73 1473 EDITION OF 1 NOV 65 IS OBSOLETE

Unclassified

SECURITY CLASSIFICATION OF THIS PAGE *(When Data Entered)*

New

410514

CONTENTS

INTRODUCTION

This research is part of a continuing study of the effects of photodetachment and photodissociation of negative ions on the production of electrons in the ionized atmosphere. Photodetachment and photodissociation cross section values are needed for the model codes to predict electron densities and ion concentrations for use in determining the electromagnetic wave transmission of normal and disturbed atmospheres. Under U.S. Army Research Office (ARO) Contract DAHC04-73-C-0016, we have previously constructed a unique experimental apparatus that enables us to measure these cross sections for thermalized ions. With this apparatus, we have measured the cross sections for a number of important atmospheric ions over the wavelength range from 4579 to 6950 Å. Under the current ARO Contract DAAG29-76-C-0023, we have extended the measurements to 8400 Å. For wavelengths in the range 5000 to 8400 Å, we have investigated all expected major atmospheric ion species, including first hydrates. The study has yielded a large number of interesting results, both for the specific atmospheric application and for the understanding of the structure and clustering mechanisms in molecular negative ions.

RESEACH RESULTS

Under the previous contract, we measured photodissociation and photodetachment cross sections for O_2^-, O_3^-, O_4^-, $O_2^- \cdot H_2O$, CO_3^-, $CO_3^- \cdot H_2O$, CO_4^-, HCO_3^- and $HCL_3^- \cdot H_2O$ at wavelengths from 4579 to 6950 Å. To completely document our knowledge gained to date of negative ion photodestruction, we have included as Appendix A a reprint of the final publication [J. Chem. Phys. 65, 5267 (1976)] summarizing the work done on the previous contract.

An obvious gap in the previous study pertained to the nitrogen-based ions, NO_2^-, NO_3^-, and their hydrates, which are very stable and important in the ionospheric chemistry. Further, both of these ions have been reported to have isomeric forms, which could play a role in their chemistry. We first investigated the photodetachment of NO_2^-. In the work reported in Appendix B, "Photodetachment and De-excitation of Excited NO_2^-" [J. Chem. Phys. 66, 4520 (1977)], we showed that NO_2^- is generally formed with substantial vibrational excitation. No evidence was found for a structural isomer of NO_2^-, and previous reports of this isomer can be reasonably attributed to the observed vibrational excitation. We also measured the vibrational de-excitation rate of $NO_2^{-\ddagger}$ by O_2, NO_2, and CO_2. These de-excitation rates are so fast that the NO_2^- found in a normal atmosphere will be largely thermalized. However, photodetachment cross sections for the excited NO_2^- were measured and could be useful in understanding the ionosphere under highly disturbed conditions. Photodetachment of thermalized NO_2^- which begins at about 5000 Å will be studied under a new contract.

Neither photodissociation nor photodetachment of normal NO_3^- would be expected to occur at the wavelengths under consideration here because of the large bond energy (4.3 eV) and electron attachment energy (3.9 eV) of this ion. However, a less stable form has been observed in ion-molecule reaction studies. It should be possible to produce this "peroxy" NO_3^- in an NO/O_2 mixture by the reaction

$$O_4^- + NO \rightarrow O_2^- \cdot NO + O_2 \quad , \tag{1}$$

but we have not yet succeeded in doing so. We have, however, produced the ion in an O_2/N_2O mixture and measured the photodissociation cross section shown in Figure 1. We have also produced the hydrate of this ion, $O_2^- \cdot NO \cdot H_2O$, and measured the photodestruction cross section shown in Figure 2. Neither the reactions leading to these ions nor their photodestruction is well

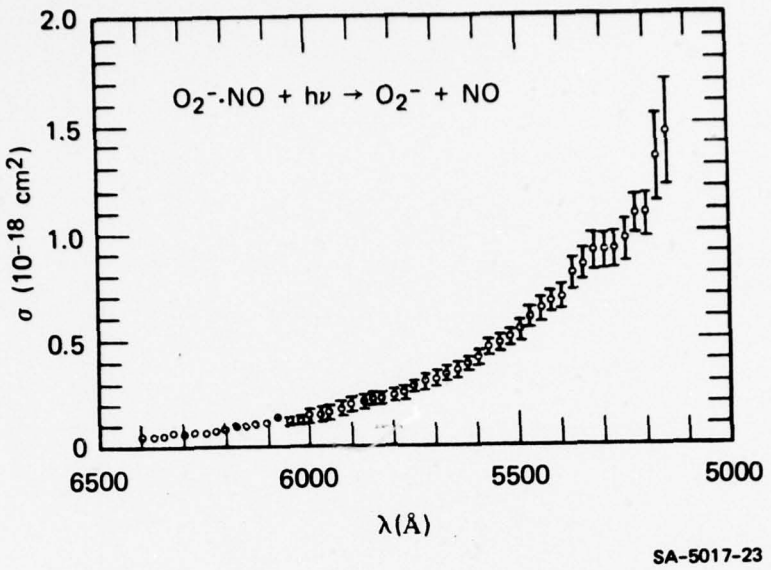

Figure 1. Photodissociation cross section for $O_2^-\cdot NO$.

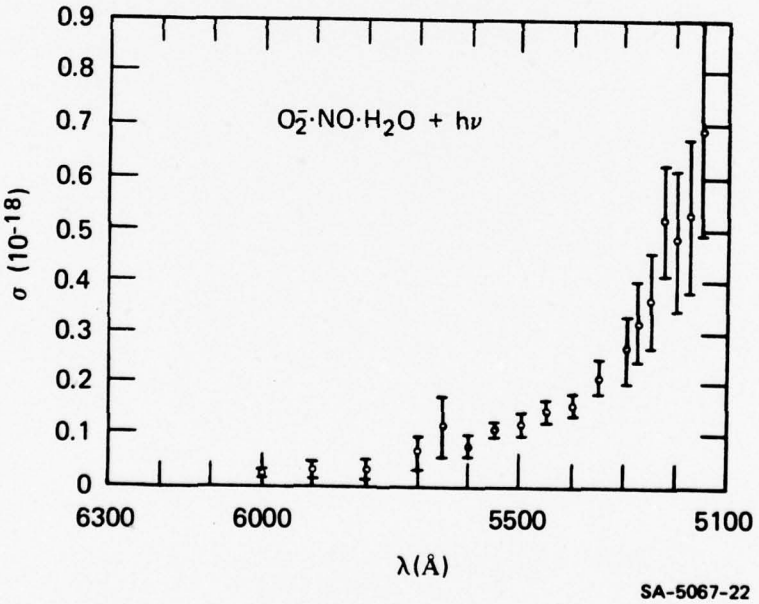

Figure 2. Photodestruction cross section for $O_2^-\cdot NO\cdot H_2O$. Destruction channels were not determined.

characterized at this time, and they will be the subject of future work. Appendix C (the abstract of a paper presented at the International Conference on the Physics of Electronic and Atomic Collisions in Paris, France, in July 1977) provides additional information on these and related ions.

The photodissociation cross section for O_3^-,

$$O_3^- + h\nu \rightarrow O^- + O_2 \quad , \tag{2}$$

shows significant structure which can be analyzed to yield vibrational frequencies for both the ground and excited state of O_3^- in a manner similar to that already done for CO_3^- [J. Chem. Phys. 65, 2512 (1976)]. The article attached as Appendix D and submitted to the Journal of Chemical Physics describes this analysis for O_3^- and discusses the identification of the dissociating state.

We have also measured the photodissociation cross sections for the first two hydrates of O_3^- and have observed them to be nearly identical with the parent ion, as discussed in Appendix E (an article submitted to the Journal of Chemical Physics).

Cross section measurements for all the ions mentioned so far were extended from 6950 to 8400 Å, using newly available infrared dyes, as described in detail in Appendix F (an article submitted to the Journal of Chemical Physics). Particularly interesting for modeling purposes is Table III of this article. This table summarizes all our negative ion photodestruction cross section measurements to date, as a function of photon energy. For ions whose cross sections are highly structured (e.g., O_3^- and CO_3^-), the structure has been smoothed so that the values in this table, when integrated over a smoothly varying photon flux, should accurately represent the photodestruction rate.

Finally, to check the accuracy of the absolute values of the cross sections, we measured the photodetachment cross sections of O^-, O_2^-, and

OH^- relative to D^-. Our cross section values reported to date have depended on normalization to a previously measured O^- cross section, whose reported accuracy is $\pm$ 10%, but which had never before been carefully checked in an independent experiment. The photodetachment cross sections for H^- and D^- can be very accurately calculated and have also been measured experimentally. This work is not yet complete, but our normalization procedure clearly is accurate to within the stated uncertainties (typically $\pm$ 20%), and, therefore, the published values can be used with confidence. It is hoped that completion of this work will decrease these uncertainties. When we have completed the measurement of the O^-, O_2^-, and OH^- cross sections relative to D^-, and performed the final assessment of the effect on our previously reported values, we will prepare an article for publication.

CONCLUSIONS

We have now measured the photodestruction cross sections for all parent negative ions believed to be important in the D-region of the ionosphere, as well as for their first hydrates, from 5100 to 8400 Å, with some measurements extending to 4579 Å. The number of photoactive ion species is very large at 5100 Å, and increases as expected toward shorter wavelengths. Further work is therefore needed to extend these measurements into the ultraviolet.

PUBLICATIONS AND CONFERENCE PRESENTATIONS

This research has resulted in four journal articles (Appendixes B, D, E, and F) and it is expected that, after some additional research, journal articles will result from the work on $O_2^- \cdot NO$ (Appendix C) and

on the measurement of the O^-, O_2^-, and OH^- photodetachment cross sections relative to D^-.

Reports on this work have been made at various conferences. Also, J. R. Peterson organized a workshop on atmospheric ion clusters at the Gaseous Electronics Conference in Cleveland, Ohio (19 through 22 October 1976). A list of conference presentations is given below.

1. J. R. Peterson, P. C. Cosby, and J. T. Moseley, "Photodestruction of Atmospheric Negative and Positive Ions," Proceedings of the COSPAR, Philadelphia, 1976 (Pergamon Press, 1977), p. 243.
2. B. A. Huber, P. C. Cosby, J. T. Moseley, and J. R. Peterson, "Photodetachment of Excited NO_2^-," Paper CB5, 29th GEC, Cleveland, Ohio (1976).
3. P. C. Cosby, J. H. Ling, J. T. Moseley, and J. R. Peterson, "Photodissociation Spectroscopy of O_3^-," Paper IA1, 29th GEC, Cleveland, Ohio (1976).
4. J. T. Moseley, "Photodissociation of Cluster Ions," Invited Paper J4, 29th GEC, Cleveland, Ohio (1976).
5. P. C. Cosby, G. P. Smith, J. H. Ling, J. R. Peterson, and J. T. Moseley, "Photodissociation of O_3^- and its Hydrates," X ICPEAC Abstracts of Papers, p. 111 (Paris, 1977).
6. P. C. Cosby, G. P. Smith, J. R. Peterson, and J. T. Moseley, "Photon Interactions Involving NO_2^-, NO_3^-, and their Hydrates," ibid; p. 113.
7. B. A. Huber, P. C. Cosby, J. R. Peterson, and J. T. Moseley, "Collisional De-excitation and Photodetachment of Excited NO_2^-," ibid; p. 115
8. J. T. Moseley, "Ion Photodissociation and Photofragment Spectroscopy," X ICPEAC Invited Papers and Progress Reports (Paris, 1977).
9. J. T. Moseley, "Photon Interactions with Molecular Ions," Paper G-2-17, 3ene Symposium International de Chimie des Plasmas, Limogis, France (1977).
10. J. T. Moseley, P. C. Cosby, and J. R. Peterson, "Photodissociation and Photodetachment Cross Sections of Atmospheric Ions," IAGA/IAMAP Symposium on Ions in the Middle Atmosphere, p. 57 (Seattle, 1977).
11. G. P. Smith, L. C. Lee, P. C. Cosby, J. R. Peterson, and J. T. Moseley, "Photodissociation Cross Sections of Atmospheric Negative Ions," Paper MA5, 30th GEC, Palo Alto, California (1977).
12. P. C. Cosby, G. P. Smith, J. T. Moseley, and L. C. Lee, "Photodissociation of Atmospheric Positive Ions," Paper MA6, ibid.
13. J. T. Moseley, P. C. Cosby, J. R. Peterson, and G. P. Smith, "Formation and Photodissociation of Peroxy NO_3^-," Paper MA7, ibid.

APPENDIX A

Photodissociation and photodetachment of molecular negative ions. III. Ions formed in $CO_2/O_2/H_2O$ mixtures*

P. C. Cosby, J. H. Ling, J. R. Peterson, and J. T. Moseley†

Molecular Physics Center, Stanford Research Institute, Menlo Park, California 94025
(Received 29 July 1976)

Total photodestruction cross sections for O_2^-, O_3^-, O_4^-, $O_2^-\cdot H_2O$, CO_4^-, CO_3^-, and $CO_3^-\cdot H_2O$ have been measured over the range from 6950 to 4579 Å (1.78–2.71 eV). In most cases the photodestruction of these ions can be attributed to specific photodissociation or photodetachment processes. The ions HCO_3^- and $HCO_3^-\cdot H_2O$ have also been investigated, and upper limits determined for their total photodestruction. The experiments were performed using a drift tube mass spectrometer coupled with an argon ion laser and a tunable dye laser. The cross section values vary from 2×10^{-20} to 1×10^{-17} cm^2, and in most cases photodissociation is the predominant process. In CO_3^- and O_3^- evidence is found for bound, predissociating excited states.

I. INTRODUCTION

In recent work[1–4] it was discovered that several ions important in the 60–90 km D region of the ionosphere undergo substantial photodissociation by visible light. Calculations[5] have shown that photodissociation is an important daytime loss mechanism for CO_3^- and $CO_3^-\cdot H_2O$ and could account for the rapid increase of electron density[6] in the D region at sunrise. Photodetachment and photodissociation processes are also important in gas discharge[7] and e-beam pumped[8] lasers, in magnetohydrodynamic generators[9], and in the study of photon-induced chemical reactions. In addition, there is fundamental interest in the interactions of photons with molecular ions. Studies of such interactions can provide information[10–15] about the location, shape and symmetry of the ground and excited states of ions, molecular bond energies, the electron affinity of the neutral parent, and energy partioning in photodissociation reactions.

In this paper we report total photodestruction cross sections over the range from 4579 to 6950 Å for a number of ions formed in mixtures of CO_2, O_2, and H_2O. The ions studied were chosen primarily for their possible importance in the D region, but the cross sections reported should also be useful in other applications. We make no attempt here at a detailed analysis of the results in terms of the structural properties of the ions, since each such analysis is quite involved and requires other experimental information in addition to the reported cross sections. In the cases of O_3^- and CO_3^-, however, such analysis is under way and is mentioned below.

II. APPARATUS AND TECHNIQUE

The experimental apparatus, which consists of a drift tube mass spectrometer, an argon ion laser, and a tunable dye laser, has been previously described[2,4] in some detail. Briefly, the negative ions are formed in the gas phase (0.050–0.400 torr) by electron attachment processes and subsequent ion–molecule reactions, and drift under the influence of a weak applied electric field through the background gas toward an extraction aperture. In these experiments, the ratio of the electric field to the neutral-gas density, E/N, is chosen such that the directed drift velocity is only about one tenth the mean thermal speed of the ions and gas molecules at room temperature. The drift distance is chosen so that the ions experience many thermalizing collisions following their production. Just before passing through the extraction aperture, the ions intersect the intracavity photons of the laser, which is chopped at 100 Hz. The ions that pass through the extraction aperture into the high vacuum analysis region are mass selected by a quadrupole mass spectrometer and individually detected by an electron multiplier.

Photons at seven discrete energies between 2.34–2.71 eV are obtained using the lines of a commercial argon ion laser. Continuously tunable photon energies between 1.78–2.43 eV are obtained using a commercial "jet-stream" dye laser pumped by the argon laser. In both cases, the drift tube is contained in the cavity of the appropriate laser. A major improvement over the earlier experiments has been achieved by using a more powerful commercial argon ion laser, having a nominal output power of 12 W (all lines) to pump the dye laser. Table I shows the dyes used, together with the wavelength range and peak intracavity powers obtained.

The wavelength of the dye laser is calibrated with a reversion spectroscope and a 0.3 m monochromator relative to the He–Ne and argon laser lines, to an accuracy of ±1 Å. In both laser configurations, the photon beam is linearly polarized perpendicular to the axis of the drift tube. The circulating power is sampled by calibrated low transmittance output couplers and monitored by a disk calorimeter.

Although, in principle, it is possible to determine absolute photodestruction cross sections in our experiment, all the cross sections reported here are put on an absolute scale by the following normalization procedure. The photodestruction cross section $\sigma(\lambda)$ for any negative ion A^- relative to the known cross section of another reference ion R^- is given by

$$\sigma_{A^-}(\lambda) = \sigma_{R^-}(\lambda)\frac{\ln(I_0/I)_{A^-}}{\ln(I_0/I)_{R^-}}\frac{P_{R^-}}{P_{A^-}}\frac{v_{A^-}}{v_{R^-}} \quad . \tag{1}$$

In this expression, I and I_0 are the numbers of ions detected at a given wavelength during the laser on and off periods, respectively, P_{R^-}/P_{A^-} is the ratio of the laser output powers measured during the accumulation of counts for each species, and v_{A^-}/v_{R^-} is the

TABLE I. Laser dyes.

Dye	Concentration[a]	Pump Lines[b]/Power(W)	Wavelength range (Å)	Cavity power (min/max, in W)	Lifetime[c] (h)
Cresyl violet[d,e]	0.001 *M* (EG) +0.0014 *M* R6*G* +0.1% COT +2% MEOH	All/16	7000–6500	19/51	5
Rhodamine *B*[e]	0.006 *M* (EG) +0.2% COT	All/16	6700–6000	42/187	24[f]
Rhodamine 6*G*[e]	0.003 *M* (EG) +0.2% COT +2% MEOH	All/16	6430–5650	40/220	Indefinite
Sodium fluorescein[e]	0.003 *M* (EG) +0.3% COT	All/16	5700–5275	17/120	Indefinite[f]
Coumarin 540[g]	0.0013 *M* (EG) +20% BA +0.2% COT	4880/8	5450–5125	13/54	36[f]

[a]Concentrations given in moles per liter (M) and percent by volume (%) for an ethylene glycol (EG) solution. R6G = rhodamine 6G dye; COT = 1,3,5,7-cyclooctatetraene; MEOH = methanol; BA = benzyl alcohol.
[b]Lines of the argon ion laser used to pump the dye.
[c]Lasing period of a 1.5 l solution of the dye over which the cavity power decreased by approximately 60%.
[d]The acetate, nitrate, and perchlorate salts of this dye have been used and are essentially equivalent in performance.
[e]Available from Eastman Kodak Co.
[f]COT must be frequently replenished to maintain performance.
[g]Equivalent to Coumarin 6. Available from Exciton Chemical Co.

ratio of mean speeds for each species when passing through the photon beam. This procedure avoids the necessity of knowing precisely the intracavity photon flux and the overlap integral between the ions and photons, both difficult quantities to determine experimentally. In many cases, the ratio v_A/v_R can also be determined much more accurately than can either of the velocities separately. A full discussion of these problems is found in Refs. 2 and 4. The absolute values of the cross sections reported here are based on a normalization to the O^- photodetachment cross section, as measured by Branscomb, Smith, and Tisone.[16]

The total photodestruction cross section in Eq. (1) describes the loss of an ion due to photodetachment or photodissociation (or both). Other mechanisms such as multiphoton processes, collisional dissociation, or reactions following photon excitation to a bound state are unlikely under our operating conditions, and we have not yet observed any such processes. Photodissociation may be observed directly by tuning the quadrupole mass filter to the mass of a photofragment ion and observing the increase in this ion when the laser is on,[1-3] or by using the difference between the mobilities of the parent and photofragment ions.[4] Photodetachment cannot be observed directly, but its presence can be inferred from differences in the photodestruction cross section and the apparent dissociation cross section obtained from observation of photofragment ions.

A particular feature of these experiments is the ability to bring the ions, that may be created in high vibrational or even excited electronic states, into thermal equilibrium with the background gas at essentially room temperature. One would expect strong effects from vibrational excitation on the photodissociation of an ion, and we have observed effects[1-4] attributed to such excitation. Due to the relatively high pressure and long drift distance of this apparatus, the ions can be made to undergo many thermalizing collisions, typically between 10^3–10^4, before the photon interaction. Often, changes in the total cross section are observed when the number of collisions is small, or when the drift velocity is larger than thermal velocity.

All results reported here were obtained under conditions such that the cross sections remained constant as the number of collisions was further increased, and all were obtained for drift velocities much less than thermal velocity. In many cases, extensive tests were made, such as those reported in Refs. 1–4, in a further attempt to detect effects of possible vibrational excitation. Therefore, except where specifically noted in the text, it is reasonable to assume that the cross sections reported here refer to a room temperature thermal distribution of vibrational levels in the parent ion. This situation differs significantly from photodissociation measurements made using fast ion beams,[11,14] where substantial vibrational excitation of the parent is observed, and where this excitation is encouraged to allow measurement of the vibrational spacings and populations in the ground state of the parent ion.

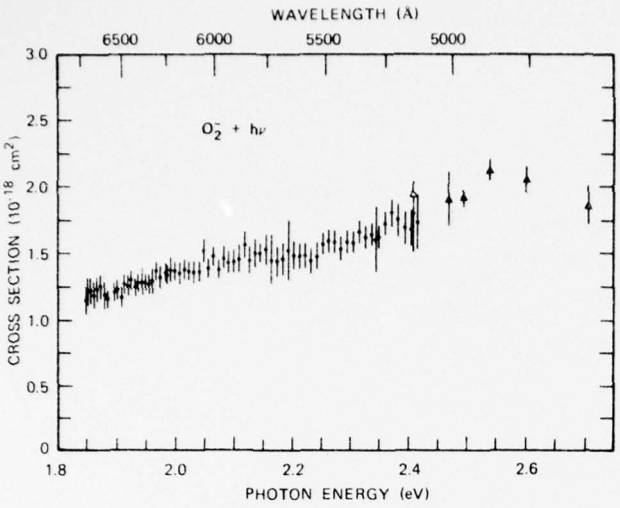

FIG. 1. Photodetachment cross section of O_2^- as a function of photon energy. The isolated error bars are the dye laser data; the triangles are data obtained at discrete argon ion laser lines.

III. PHOTODETACHMENT OF O_2^-

The O_2^- ions used for these measurements were produced in pure O_2 gas at a pressure of 0.1 torr, primarily by the three-body attachment reaction

$$e^- + O_2 + O_2 \rightarrow O_2^- + O_2 \ . \tag{2}$$

The measurements were made using a drift distance of at least 10.2 cm and an E/N of 10 Td (1 townsend = 10^{-17} V cm^2). Under these conditions only O^- and O_2^- ions were observed in significant concentrations. Small amounts of O_3^- and CO_3^-, less than 1 part in 10^3 of the O^- and O_2^- intensities, could also be observed.

Earlier measurements[4] on the photodetachment of O_2^- have been extended to cover a much wider wavelength range. The results are shown in Fig. 1 as a function of photon energy. The photodestruction here is clearly photodetachment, since the bond energy of O_2^- is greater 4 eV. The present results differ slightly from the earlier ones, between 6400–5650 Å but agree within the combined uncertainties. The present results show a smoother cross section with less possibility of the structure that was suggested earlier.[4] The absolute values are in excellent agreement with the measurements of Burch, Smith, and Branscomb,[17] who used a fast ion beam and color filters to select photon energies with a bandwidth of approximately 0.2 eV; with those of Warneck,[18] who also used a fast ion beam, but with a monochromator to obtain a photon energy resolution of 0.07 eV; and with very recent measurements of Vanderhoff and Beyer,[19] who used the discrete lines from argon and krypton lasers and a drift tube mass spectrometer technique similar to the one used here. The photon energy resolution in the present experiment is about 0.0003 eV.

The error bars given in Fig. 1 represent the root-mean-square sum of the statistical uncertainties in the measurement of $\ln(I_0/I)$ and the relative power terms in Eq. (1). Contributions to the uncertainty in the absolute scale consist of a 10% uncertainty in the value of the O^- photodetachment cross section, and a 4% uncertainty in the velocity ratio. Consequently, the absolute scale is considered accurate to ±12%.

IV. PHOTODISSOCIATION OF O_3^-

The O_3^- ions used in this study were produced in pure O_2 gas at pressures ranging from 0.2 to 0.4 torr, E/N of 10 Td, and drift distances of at least 10.2 cm, by the reaction[20–22]

$$O^- + 2O_2 \rightarrow O_3^- + O_2 \ . \tag{3}$$

As has been discussed,[4] it is energetically possible for O_3^- to photodetach and to photodissociate via the reaction

$$O_3^- + h\nu \rightarrow O^- + O_2 \tag{4}$$

at the photon energies used here.

The results of the total photodestruction measurements of O_3^- are given in Fig. 2 as a function of photon energy. As discussed in Ref. 4, comparison of the loss of O_3^- with the appearance of O^- photofragment ions indicates that (85% ± 15%) of the observed photodestruction occurs by the photodissociation process of Eq. (4). In addition, the measurements of the photodetachment cross section of O_3^- by Wong, Vorburger, and Woo[23] indicate that photodetachment contributes less than 10% to the total photodestruction shown in Fig. 2 at photon energies above 2.1 eV. To avoid the difficulties associated with normalizing the O_3^- cross section to O^-, when the O^- is not only destroyed by photodetachment but also produced in the photodissociation of O_3^-, the cross sections were normalized to those of O_2^- reported in the preceding section. The error bars in Fig. 2 were calculated as for O_2^-, but include the additional uncertainty in the O_2^- cross section. The uncertainty in the absolute scale is again ±12%.

This cross section shows a series of broad peaks and some subsidiary structures. Several researchers[24–27] have observed an absorption in O_3^- trapped in different solid environments in this wavelength range, with the absorption peaks spaced similarly to the observed broad peaks in the photodestruction cross section. Similar peaks have also been observed in the relative photodestruction measurements of O_3^- by Sinnott and Beaty.[28] We have previously discussed briefly[4] the possible interpretation of our earlier results on O_3^-. These new results will allow a more detailed analysis of this process and of the electronic states of O_3^-. The results of this investigation will be reported separately.

V. PHOTODESTRUCTION OF O_4^-

The O_4^- ions used in this study were produced in pure O_2 gas at pressures ranging from 0.3 to 0.4 torr, an E/N of 10 Td, and drift distances of at least 10.2 cm. The O_4^- ions are formed in the reaction

$$O_2^- + O_2 + O_2 \rightleftharpoons O_4^- + O_2 \ , \tag{5}$$

for which the forward and reverse rate constants have

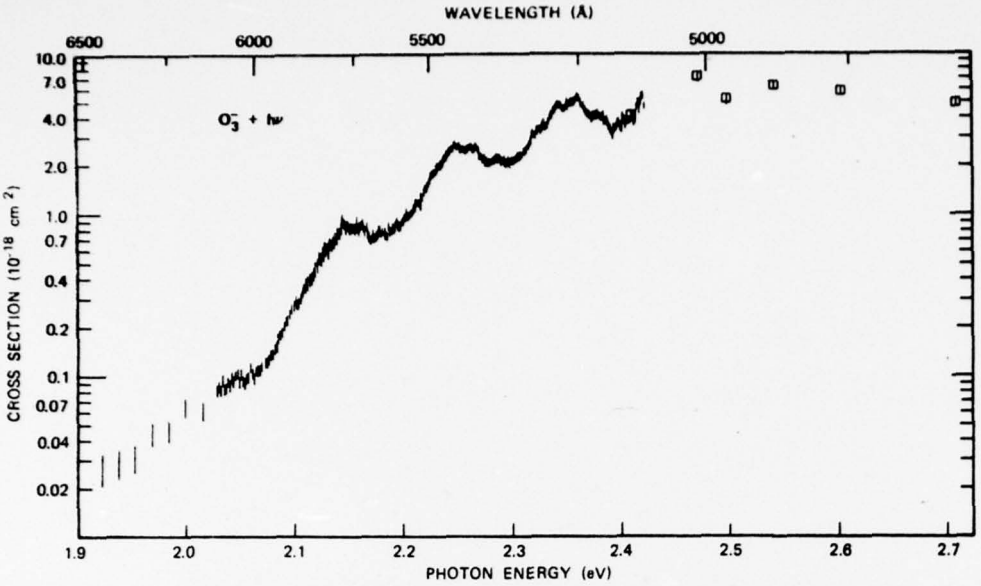

FIG. 2. Photodestruction cross section of O_3^- as a function of photon energy. The isolated error bars are the dye laser data; the squares are data obtained at discrete argon ion laser lines.

been measured[21,22] to be $4-5.1\times10^{-31}$ cm^6 sec^{-1} and $1.6-2.7\times10^{-14}$ cm^3 sec^{-1}, respectively. Thus, at the gas densities used here ($1.0-1.3\times10^{16}$ cm^{-3}), O_4^- ions are formed continuously along the drift path between the source and the laser beam. It should, therefore, not be assumed that these ions are in thermal equilibrium with the gas. However, the observed photodestruction cross section for O_4^- was found to be independent of variations in drift distance from 5.1 to 25.4 cm, and of variations in pressures from 0.3 to 0.4 torr, indicating either that the cross section may be insensitive to the internal energy of the O_4^- or that any internal excitation produced in the formation of O_4^- is rapidly quenched.

Total photodestruction cross sections for O_4^- are given in Fig. 3 as a function of photon energy. These cross sections were put on an absolute scale by normalization to the O_2^- cross sections of Fig. 1. The large number of O_3^- ions always present under the conditions used to form O_4^- prevents direct normalization to O^-. Of course, O_4^- might also photodissociate, yielding O_2^-, since the heat of formation of O_4^- is only 0.6 eV.[29] However, the effect of this process on the normalization would be negligible since the concentration of source-produced O_2^- in the photon interaction region is two orders of magnitude greater than that of O_4^-. The error bars in Fig. 3 again represent the statistical uncertainties, plus the relative uncertainty of the O_2^- cross section used for normalization. The uncertainty in the absolute scale is ±15%, including the uncertainty in the absolute O_2^- cross sections and in the velocity ratio.

Energetically, O_4^- may photodissociate and photodetach. Efforts to observe the production of photofragment ions were unsuccessful because of the large number of O^-, O_2^-, and O_3^- ions in the photon interaction region, compared with O_4^-, and because of the similar drift velocities[30] of the O_2^-, O_3^-, and O_4^- ions. The strong similarity between the O_4^- photodestruction cross section and the O_2^- photodetachment cross section is noted; the two are in fact equal within their mutual uncertainties at energies above 2.0 eV. The photodestruction mechanism for this ion can be determined by using substantially higher pressures to increase the relative O_4^- population or by conducting a beam experiment[11,14] and would probably help greatly in understanding the nature of the $O_2\cdot O_2^-$ bonding in this ion. In any case, photodestruction must result in dissociation, since O_4 is not stable.

VI. PHOTODESTRUCTION OF $O_2^-\cdot H_2O$

The $O_2^-\cdot H_2O$ ions were formed by the reaction[21,22]

$$O_2^- + H_2O + M \rightarrow O_2^-\cdot H_2O + M\,, \qquad (6)$$

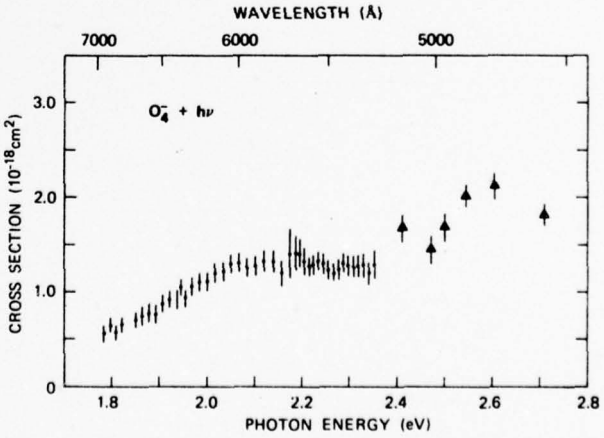

FIG. 3. Photodestruction cross section of O_4^- as a function of photon energy. The isolated error bars are the dye laser data; the triangles are data obtained at discrete argon ion laser lines.

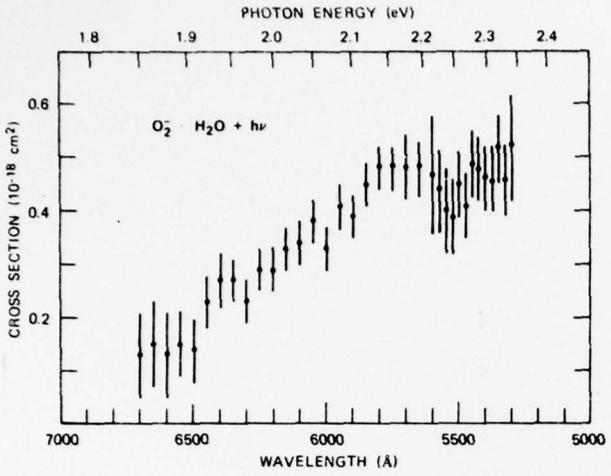

FIG. 4. Photodestruction cross section of $O_2^- \cdot H_2O$ as a function of photon wavelength.

in a 98:2 mixture of O_2 and H_2O at a total pressure of 0.1 torr, an E/N of 10 Td, and drift distances of at least 10.2 cm. The results are presented in Fig. 4 as a function of wavelength. The uncertainties were determined as for O_4^-, and the uncertainty in the absolute scale is again ±15%. Also, as in the O_4^- case, it is not asserted that the $O_2^- \cdot H_2O$ ions were in thermal equilibrium with the gas when they passed through the laser beam; nor was the photodestruction channel determined. Again, both photodetachment and photodissociation are energetically possible, and photodetachment will yield dissociation into O_2, H_2O, and an electron.

VII. PHOTODISSOCIATION OF CO_3^-

The CO_3^- ions used in this study were formed in pure CO_2 gas, and in mixtures of O_2 and CO_2, at a pressure of 0.050 torr, an E/N of 10 Td, and a drift distance of at least 10.2 cm. The formation, equilibration, and photodestruction processes have been extensively discussed[1-3] and will not be repeated here. It is concluded that the results, presented in Fig. 5, are for the photodissociation of CO_3^-, which is in thermal equilibrium at room temperature, by the process

$$CO_3^- + h\nu \rightarrow O^- + CO_2 \,. \tag{7}$$

The absolute scale was determined by normalization to both O^- and O_2^- and has an uncertainty of ±15%.

We have noted[3] that the structure in this cross section reflects the vibrational levels of a bound, predissociating state of CO_3^-. We have recently made a detailed analysis[31] of the CO_3^- spectrum, and summarize the results here for completeness. The bond energy $D(CO_2-O^-)$ is (1.8±0.1) eV, and the electron affinity E. A. (CO_3) is (2.9±0.3) eV. Assuming the ground state of CO_3^- is $^2B_2$, the excited state responsible for the observed structure is $^2A_1$. The three bending modes of this state have frequencies of 990, 1470, and 880 cm^{-1}, and the ground level of this state is 1.520 eV above the ground level of the ground state.

VIII. PHOTODISSOCIATION OF $CO_3^- \cdot H_2O$

The $CO_3^- \cdot H_2O$ ions were formed using two different gas mixtures. A mixture of CO_2 and H_2O at 0.05 torr, with a H_2O concentration of less than 1% (by volume), at an E/N of 10 Td and a drift distance of 5.1 cm or greater, produced the ions O^-, CO_3^-, $CO_3^- \cdot H_2O$, OH^-, HCO_3^-, and $HCO_3^- \cdot H_2O$. Higher hydrates of CO_3^- and HCO_3^- could be observed only at significantly higher H_2O concentrations (>10%). A mixture of O_2, CO_2, and H_2O was also used in this work. The concentration of CO_2 was maintained at approximately 5%, while that of H_2O was less than 1%. At an E/N of 5 or 10 Td, a drift distance of 20.3 cm, and a total pressure of 0.1 or 0.15 torr, O_2^- and traces of $O_2^- \cdot H_2O$ were formed in addition to those ions observed in the CO_2-H_2O mixture.

The $CO_3^- \cdot H_2O$ is formed in the three-body reaction[32]

$$CO_3^- + H_2O + M \rightarrow CO_3^- \cdot H_2O + M \,. \tag{8}$$

Observations of the arrival time spectra of the ions when the source was pulsed and of the photodestruction behavior of each of the ions revealed no evidence of ion–molecule reactions or of photon interactions coupling the ions based on O^- (CO_3^- and its hydrates) and those based on OH^- (HCO_3^- and its hydrates). In the CO_2-H_2O mixture, the total photodestruction cross section for $CO_3^- \cdot H_2O$ could be measured relative to the CO_3^- cross section with negligible interference[2] from other photodestruction processes when proper account was taken of photofragment CO_3^- ions. In the $O_2-CO_2-H_2O$ mixtures, the $CO_3^- \cdot H_2O$ cross section could be mea-

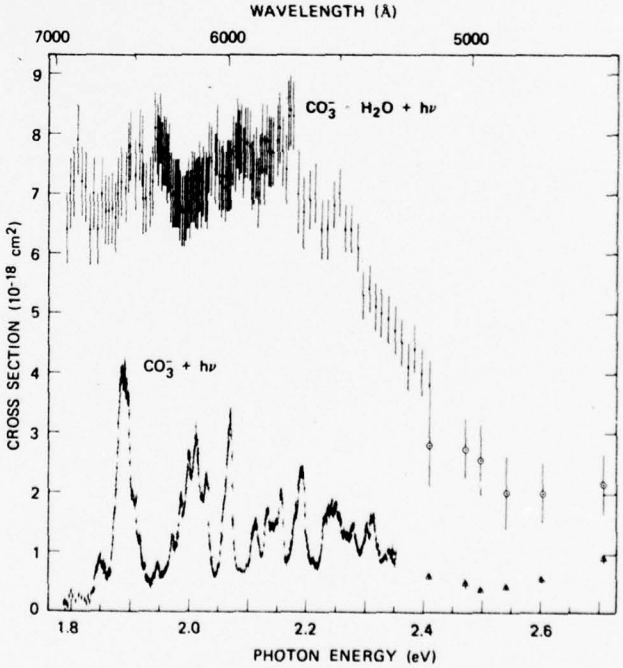

FIG. 5. Total photodestruction cross sections of CO_3^- (lower) and $CO_3^- \cdot H_2O$ (upper) as a function of photon energy. The open triangles and open circles are data obtained at discrete argon ion laser lines for CO_3^- and $CO_3^- \cdot H_2O$, respectively; the isolated error bars are the dye laser data.

sured relative to that of O_2^- with no measurable interference of photofragment ions.

The results of the $CO_3^- \cdot H_2O$ photodestruction measurements are given in Fig. 5. The error bars include the statistical uncertainties in $\ln(I_0/I)$, in the relative power measurement, and in the CO_3^- and O_2^- cross sections used for normalization. The uncertainty in the absolute scale is $\pm 20\%$, reflecting the absolute uncertainties in the CO_3^- and O_2^- cross sections and in the ratios of the relative velocities of these ions to that of $CO_3^- \cdot H_2O$.

Since the electron affinity of CO_3 is (2.9 ± 0.3) eV and the electron attachment energy of $CO_3^- \cdot H_2O$ will exceed that of CO_3^- by approximately the $CO_3^- \cdot H_2O$ bond energy (~ 0.5 eV), the observed photodestruction of $CO_3^- \cdot H_2O$ must be photodissociation.

Dissociation into $CO_3^- + H_2O$ and $O^- \cdot H_2O + CO_2$ should be energetically permitted over the entire wavelength range used here. In addition, the threshold for dissociation into $O^- + CO_2 + H_2O$ would be expected at 5500 Å or shorter wavelengths, given the bond energies involved.

We have searched for the production of these photofragment ions at wavelengths between 5145–6400 Å. In this region only CO_3^- photofragments were observed, and in amounts that accounted for $90\% \pm 10\%$ of the total $CO_3^- \cdot H_2O$ photodestruction. No evidence was observed for the production of O^- or $O^- \cdot H_2O$ photofragments by the hydrate. However, it is known[32] that the $O^- \cdot H_2O$ ion reacts rapidly ($k > 1 \times 10^{-11}$ cm^3/sec) in oxygen gas, and it is likely that a similar reaction will take place in CO_2 at about the same or even faster rate. For the drift tube conditions used here, more than half (and possibly all) of any photofragment $O^- \cdot H_2O$ would consequently be destroyed by reaction prior to their detection. It is similarly difficult to assess the possible production of photofragment O^- from $CO_3^- \cdot H_2O$. For the drift tube conditions used here, the maximum number of photofragment O^- ions that could possibly be produced from the hydrate (i.e., $\leq 20\%$ of the total $CO_3^- \cdot H_2O$ photodestruction) would be two orders of magnitude smaller than the number of photofragment O^- ions that are simultaneously produced from CO_3^-. Moreover, the nearly identical mobilities of CO_3^- and $CO_2^- \cdot H_2O$ do not permit resolution of their respective photofragments using time-of-flight techniques. We therefore conclude that although photodissociation of $CO_3^- \cdot H_2O$ to form either O^- or $O^- \cdot H_2O$ photofragments cannot be entirely ruled out, the predominant photodissociation channel at visible wavelengths yields $CO_3^- + H_2O$.

We have previously[2] discussed several possible interpretations of the $CO_3^- \cdot H_2O$ photodestruction at the argon laser lines. The cross section obtained using the dye laser and our interpretation of the CO_3^- results[31] now allow a better understanding of the $CO_3^- \cdot H_2O$ photodissociation. We have concluded that CO_3^- absorbs at photon energies between 1.52–2.35 eV into a state that is predissociative above 1.8 eV. Above 2.35 eV, CO_3^- continues to absorb, although less strongly, probably into one or more other predissociating states. Between 1.8–2.35 eV, only three modes of CO_3^-, identified as bending modes, are found to predissociate, but it is likely that absorption also occurs into both the symmetric and antisymmetric stretch modes of the excited electronic state. If the weak $CO_3^- - H_2O$ bond (~ 0.5 eV)[32] is primarily electrostatic, the presence of the H_2O should only slightly perturb the electronic states of the isolated CO_3^- ion. Thus, photoabsorption by the hydrate should take place over essentially the same range of photon energies as for CO_3^-. But when the cluster absorbs, in addition to radiation back to the ground state or dissociation into O^- or $O^- \cdot H_2O$, it has a lower energy channel for disposing the energy acquired in the photoabsorption—ejection of the H_2O.

It is seen in Fig. 5 that the similarity in the energy dependences of the mean destruction cross section for the CO_3^- and $CO_3^- \cdot H_2O$ ions at photon energies above approximately 1.9 eV supports this model, as does the fact that $CO_3^- \cdot H_2O$ continues to dissociate at energies below the photodissociation threshold of the CO_3^-. It is therefore expected that the threshold for the hydrate photodissociation will occur in the region of the predicted origin of the 1^2A_1 state of CO_3^- at 1.52 eV. The actual threshold will depend on the relative interactions of the H_2O with the ground and excited CO_3^- states. It is not now understood how the photoexcited levels in the region of 1.8 eV, which are only about 0.3 eV above the ground level of the 1^2A_1 state of CO_3^-, are effective in supplying the $\simeq 0.5$ eV required to dissociate the H_2O cluster. Certainly there is sufficient electronic energy, and it may be that radiationless transitions to vibrationally excited levels of the ground electronic state occur, which are then partly internally relaxed by dissociation into $CO_3^- + H_2O$.

The fact that the photodissociation cross section for $CO_3^- \cdot H_2O$ is substantially greater than that for CO_3^- can be explained if it is easier for the excited complex to localize 0.5 eV for ejection of the H_2O than for CO_3^- to localize 1.8 eV for the ejection of O^-. Thus the predissociation channel can compete more effectively with the radiation (fluorescence) channel in the hydrate than in the parent.

The fact that the $CO_3^- \cdot H_2O$ destruction cross section does not exhibit the same detailed structure as CO_3^- may result from additional vibrational modes that are excited by absorption but which do not contribute to dissociation in CO_3^- itself. It may also be expected that the CO_3^- absorption frequencies in the hydrate are slightly dependent on the orientation of the water molecule and that the vibrational excitation present in the $CO_3^- \cdot H_2O$ bound at 300 °K thus causes absorption spectrum of the hydrated CO_3^- to be smoothed out compared with that of CO_3^-.

The presence of the water molecule (and its associated electric dipole field) may also increase the CO_3^- absorption cross section, thus accounting for the three times larger destruction cross section in the hydrate. Since it is unlikely that changes in the Franck–Condon factors alone could lead to such an increase, this effect would require a change in the oscillator strengths of the transitions. In view of the close similarity of

TABLE II. Total photodestruction cross section of CO_4^-.

Wavelength (Å)	Cross section (10^{-20} cm^2)
6900	< 3.0
6500	< 1.6
6400	< 2.0
6200	< 2.0
6000	< 2.1
5800	< 2.8
5500	< 2.0
5200	2.5 ± 2.3
5145	3.7 ± 2.0

the envelopes of the two cross sections, indicating that the absorbing levels of the hydrate are essentially those of the isolated CO_3^-, this explanation is not very convincing.

While this discussion is clearly not definitive, the present results do allow a narrowing of the alternatives proposed earlier[2] and suggest additional experiments that should assist in our understanding of $CO_3^- \cdot H_2O$ and its photodestruction characteristics.

IX. PHOTODESTRUCTION OF HCO_3^- AND $HCO_3^- \cdot H_2O$

As mentioned in the preceding section, addition of H_2O to CO_2 in the drift tube results in the production of OH^-, HCO_3^-, and hydrates of HCO_3^-. Alternatively, the HCO_3^- ion can be produced[32] in the absence of hydrates by using a 98 : 2 mixture of CO_2 and CH_4. We have investigated the total photodestruction cross section of HCO_3^- by each method of formation, using the tunable dye laser at wavelengths between 6500–5145 Å. We found that the cross section for this ion is less than 3×10^{-20} cm^2 over this wavelength range, and possibly zero.

Results for $HCO_3^- \cdot H_2O$ were similar to those for HCO_3^-. The total photodestruction cross section was observed to be less than 7×10^{-21} cm^2 at 5145 Å, and statistically consistent with zero over the range from 6500–4579 Å.

We have previously reported[2] small but nonzero photodestruction cross sections for HCO_3^- at four argon ion wavelengths. However, in the course of our further work using the drift tube, we found that the photon beam produced a small modulation (< 0.1%) of the detected current of a nonabsorbing ion species when it was in the presence of relatively high densities of other species that have large photodestruction cross sections. We believe that this modulation results from the large changes in ion density that occur in the photon interaction region when significant fractions of the absorbing ions in this region are photodetached. This effect can be identified by monitoring the apparent photodestruction cross section as a function of total ion density. The modulation is found to occur for HCO_3^- at the dye laser wavelengths because of the high relative densities of O^- and OH^- ions present in both the CO_2–H_2O and CO_2–CH_4 mixtures. The total photodestruction cross sections reported here were obtained at a sufficiently low ion density that the modulation effect was undetectable. This precaution was not taken when the cross sections were measured at the argon ion laser wavelengths. Consequently, those values[2] should be considered only as upper limits to the HCO_3^- total photodestruction cross section, until the cross section at the argon ion laser wavelengths can be investigated as a function of total ion density.

X. PHOTODESTRUCTION OF CO_4^-

The CO_4^- studied here was formed[32] in a 95 : 5 mixture of O_2 and CO_2 at a pressure of 0.1 torr, an E/N of 5 Td, and a drift distance of 30.5 cm. This ion has an electron affinity[33] of 1.22 eV and a CO_2–O_2^- bond energy[33] of 0.8 eV. It therefore is energetically possible for it to both photodissociate and photodetach at these photon energies. The total photodestruction cross section of CO_4^- was measured at wavelengths between 6900–5145 Å, using the tunable dye laser, and at 5145 Å, using the argon ion laser.

The results, summarized in Table II, show that the cross section is less than 3×10^{-20} cm^2 at wavelengths between 6900–5500 Å. However, small but nonzero cross sections are measured at 5200 and 5145 Å. Because of the small size of these cross sections and the low abundance of CO_4^- produced in the drift tube, possible photofragments of CO_4^- could not be observed. Thus it is not known whether the photodestruction of this ion is due to photodetachment or to photodissociation.

XI. SUMMARY AND CONCLUSIONS

Photon interactions with nine molecular negative ions have been studied over the wavelength range from 6950 to 4579 Å. For three of these ions, O_3^-, CO_3^-, and $CO_3^- \cdot H_2O$, photodissociation into an ionic photofragment was observed, and evidence was obtained for the existence of bound, predissociative states in these species. For three ions, O_4^-, $O_2^- \cdot H_2O$, and CO_4^-, photodestruction was observed, which probably results in dissociation, but it was not determined whether photofragment ions were produced or neutral products and an electron. One ion, O_2^-, which can only photodetach at these wavelengths, yielded absolute values in agreement with earlier work. Two ions, HCO_3^- and $HCO_3^- \cdot H_2O$, apparently neither photodetach or photodissociate over this wavelength range.

The initial motivation for these studies was the importance of these ions in the ionosphere. However, it is apparent that these measurements provide valuable information for studies of ionic structure and potential surfaces. Such a study has been done[28] for CO_3^-, and one is under way for O_3^-. Application of ion photofragment energy spectroscopy[11,14] to ions such as CO_3^- and O_3^- should further extend our knowledge of their structure and dissociation mechanisms.

*This research was supported by the U. S. Army Ballistics Research Laboratories through the U. S. Army Research Office.

†Address for 1975–76 academic year: Laboratoire des Collisions Ioniques, Université de Paris-Sud, 91405 Orsay, France.

[1]J. T. Moseley, R. A. Bennett, and J. R. Peterson, Chem. Phys. Lett. **26**, 288 (1974).
[2]J. T. Moseley, P. C. Cosby, R. A. Bennett, and J. R. Peterson, J. Chem. Phys. **62**, 4826 (1975).
[3]P. C. Cosby and J. T. Moseley, Phys. Rev. Lett. **34**, 1603 (1975).
[4]P. C. Cosby, R. A. Bennett, J. R. Peterson, J. T. Moseley, J. Chem. Phys. **63**, 1612 (1975).
[5]J. R. Peterson, J. Geophys. Res. **81**, 1433 (1976).
[6]R. P. Turco and C. F. Sechrist, Radio Sci. **7**, 717 (1972); R. P. Turco, *ibid.* **9**, 655 (1974).
[7]W. L. Nighan and W. J. Wiegand, Phys. Rev. A **10**, 922 (1974).
[8]D. L. Huestis *et al.*, "*Visible Absorption by Rare Gas Molecular Ions and Excimers*," Paper RN4, 31st Symposium on Molecular Structure and Spectroscopy, Ohio State University, 1976.
[9]F. E. Spencer, J. C. Hendrie, and D. Bienstock, Paper VIII 4, 13th Symposium on Engineering Aspects of Magnetohydrodynamics, Stanford University, 1973.
[10]G. H. Dunn, Phys. Rev. **172**, 1 (1968).
[11]N. P. F. B. van Asselt, J. G. Mass, and J. Los, Chem. Phys. Lett. **24**, 555 (1974); Chem. Phys. **5**, 429 (1974); **11**, 253 (1975).
[12]G. E. Busch and K. R. Wilson, J. Chem. Phys. **56**, 3638 (1972).
[13]R. N. Zare, Ph.D. thesis, Harvard University, 1964; Mol. Photochem. **4**, 1 (1972).
[14]J. B. Ozenne, D. Pham and J. Durup, Chem. Phys. Lett. **17**, 422 (1972); J. B. Ozenne, J. Durup, R. W. Odom, C. Pernot, A. Tabche-Fouhaille, and M. Tadjeddine, Chem. Phys. **16**, 75 (1976).
[15]G. E. Busch and K. R. Wilson, J. Chem. Phys. **56**, 3626 (1972).
[16]L. M. Branscomb, S. J. Smith, and G. Tisone, J. Chem. Phys. **43**, 2906 (1965).
[17]D. S. Burch, S. J. Smith, and L. M. Branscomb, Phys. Rev. **112**, 171 (1958).
[18]P. Warneck, Laboratory Measurements of Photodetachment Cross Sections of Selected Negative Ions GCA Tech. Rept. 69-13-N, GCA Corp., Bedford, Massachusetts, 1969.
[19]J. A. Vanderhoff and R. A. Beyer, Bull. Am. Phys. Sec. **21**, 85 (1976); J. Chem. Phys. (in press).
[20]R. M. Snuggs, D. J. Volz, I. R. Gatland, J. M. Schummers, D. W. Martin, and E. W. McDaniel, Phys. Rev. A **3**, 487 (1971).
[21]J. L. Pack and A. V. Phelps, Bull. Am. Phys. Soc. **16**, 214 (1971).
[22]J. D. Payzant and P. Kebarle, J. Chem. Phys. **56**, 3482 (1972).
[23]S. F. Wong, T. V. Vorburger and S. B. Woo, Phys. Rev. A **5**, 2598 (1972).
[24]M. E. Jacox and D. E. Milligan, J. Mol. Spectry. **43**, 148 (1972); Chem. Phys. Lett. **14**, 518 (1972).
[25]P. A. Giguere and K. Herman, Can. J. Chem. **52**, 3941 (1974).
[26]J. B. Bates and J. C. Pigg, J. Chem. Phys. **62**, 4227 (1975).
[27]L. Andrews, J. Chem. Phys. **63**, 4465 (1975).
[28]G. Sinnott and E. C. Beaty, *Seventh International Conference on the Physics of Electronic and Atomic Collisions, Abstracts of Papers* (North Holland, Amsterdam, 1971), p. 176. Also E. C. Beaty (private communication).
[29]D. C. Conway and L. E. Nesbitt, J. Chem. Phys. **48**, 509 (1968).
[30]R. M. Snuggs, D. J. Volz, J. H. Schummers, D. W. Martin, and E. W. McDaniel, Phys. Rev. A **3**, 477 (1971).
[31]J. T. Moseley, P. C. Cosby, and J. R. Peterson, J. Chem. Phys. **65**, 2512 (1976).
[32]F. C. Fehsenfeld and E. E. Ferguson, J. Chem. Phys. **61**, 3181 (1974).
[33]J. L. Pack and A. V. Phelps, J. Chem. Phys. **45**, 4316 (1966).

APPENDIX B

Photodetachment and de-excitation of excited NO_2^- *

B. A. Huber,† P. C. Cosby, J. R. Peterson, and J. T. Moseley

Molecular Physics Center, Stanford Research Institute, Menlo Park, California 94025
(Received 20 January 1977)

The photodetachment of excited NO_2^- formed by charge exchange of O^- and O_2^- with NO_2 has been studied at photon energies of 1.97 to 2.34 eV, below the electron affinity of NO_2 (2.36 ± 0.10 eV). These data indicate that the subthreshold photodetachment takes place from excited vibrational levels of the NO_2^- ground electronic state, which are populated by the ion–molecule reactions producing this species. De-excitation of the excited NO_2^- is observed in collisions with O_2 and CO_2 molecules with apparent rates in the range of 10^{-12} cm^3/sec and with NO_2 molecules at a rate of nearly 10^{-9} cm^3/sec. The absolute photodetachment cross section of nascent NO_2^- is determined at three photon energies. No evidence is found for a structural (peroxy) isomer of this ion.

I. INTRODUCTION

The NO_2^- ion plays an important role as an intermediate in the chemistry of the *D*-region of the ionosphere,[1] where it is formed primarily by the reaction

$$CO_3^- + NO \rightarrow CO_2 + NO_2^-. \quad (1)$$

Knowledge of the photodetachment and photodissociation cross sections of NO_2^- is important[1] in assessing the loss mechanisms of NO_2^- in the aeronomic ion scheme. The electron affinity of nitrogen dioxide has been determined by different techniques[2–4]; recent photodetachment measurements[5] of NO_2^- have yielded a value of 2.36 ± 0.10 eV, in agreement with the older data. Because of the large dissociation energy of NO_2^- (4.1 eV),[6] the photodestruction of the ground state NO_2^- in the ionosphere will occur primarily by photodetachment.

However, laboratory studies[7] of the equilibrium of reaction (1) have indicated that the NO_2^- products are formed in excited states and appear to retain a large part of their internal energy through at least several hundred collisions in O_2 to undergo the reverse reaction, which is endothermic for ground state species. This observation was supported by photodetachment studies,[5,8] in which two thresholds were found, leading to the suggestion that NO_2^- may have two structural isomers: the normal $C_{2v}(ONO^-)$, and a higher energy peroxy (NOO^-) form. In addition, no interconversion of the two species was observed.

Further support for the existence of two isomers of NO_2^- was given by an *ab initio* SCF calculation,[9] which predicted a stable peroxy form. This calculation also found a higher energy triangular form which was 4.35 eV above the normal form and 1.2 eV above the isomeric NO_2^-. Since isomerization of the normal and peroxy forms would presumably occur through the triangular intermediate, the large calculated energy barrier was consistent with the experimental observation[5,8] of the stability of the excited NO_2^-.

Since the higher energy species could play a major role in the photodestruction of NO_2^- in the ionosphere, it is of interest to determine more precisely the properties of this excited state. We have therefore studied photodetachment and deexcitation of excited NO_2^- at photon energies between 1.97 and 2.34 eV. Photodetachment of ground state NO_2^- should begin above 2.36 eV, but might begin as low as 2.26 eV. The results suggest that the excited form of NO_2^- observed here (and quite possibly in previous experiments) is the normal C_{2v} produced in excited vibrational levels rather than an isomeric form. The measured deexcitation rates and photodetachment cross sections will assist in assessing the importance of this excited NO_2^- in the ionosphere and other ionized gases.

II. EXPERIMENTAL PROCEDURES

The experiments were performed using a drift tube mass spectrometer and a tunable dye laser pumped by an argon ion laser; the apparatus has been previously described[10,11] in some detail. The NO_2^- ions, formed in an electron impact ion source, drift under the influence of a weak electric field toward the extraction aperture. The ratio of the electric field *E* and the neutral density *N* was 10 Td, (1 Td = 10^{-17} V cm^2), assuring that the drift velocity of the NO_2^- ions was much smaller than the mean thermal speed of the ions at room temperature. Before exiting the drift region, the ions intersect the chopped laser beam. After passing through the extraction aperture, they are mass selected by a quadrupole mass spectrometer and detected by a channeltron electron multiplier. The photodestruction cross section for NO_2^- was determined by counting the ions of this mass for alternate periods with the laser on and off, and is put on an absolute scale by normalization to the photodetachment cross section of O_2^-.[11] As will be discussed, the NO_2^- ions were formed in a number of different gas mixtures at a total pressure of 0.1 torr. The majority of the measurements were performed in oxygen containing various small amounts of NO_2, but studies were also done in oxygen containing N_2, CO_2, and NO. When NO was used, a small but unknown amount of NO_2 was present despite additional purification.

III. RESULTS

In the following we will discuss primarily the results for the NO_2–O_2 mixture, since for the other gas mixtures neither the formation scheme for the NO_2^- ions nor the gas composition is accurately known. The principal features of the NO_2^- photodetachment cross section observed in each of these mixtures are qualitatively the same, however.

When a small amount of NO_2 (<1%) is added to the drift tube containing O_2 at a pressure of 0.1 torr and a

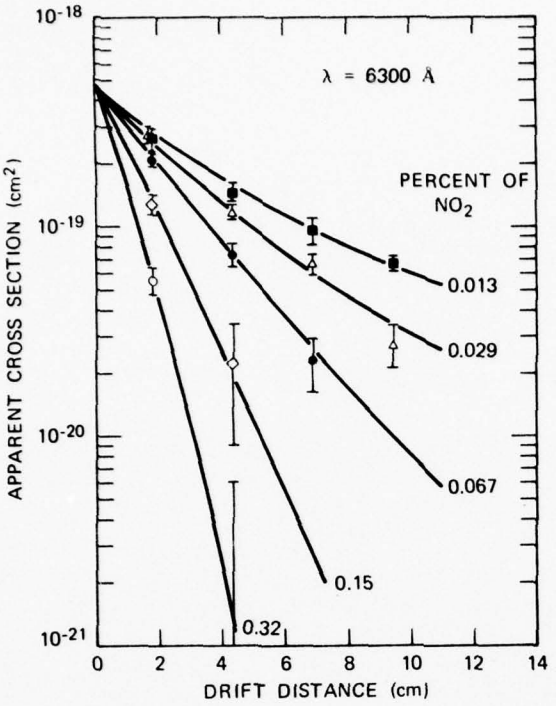

FIG. 1. Apparent photodetachment cross section of NO_2^- as a function of the drift distance at a photon energy of 1.95 eV (6300 Å). The solid curves are calculated from the two level model for different NO_2 concentrations in O_2, corresponding to the experimental values.

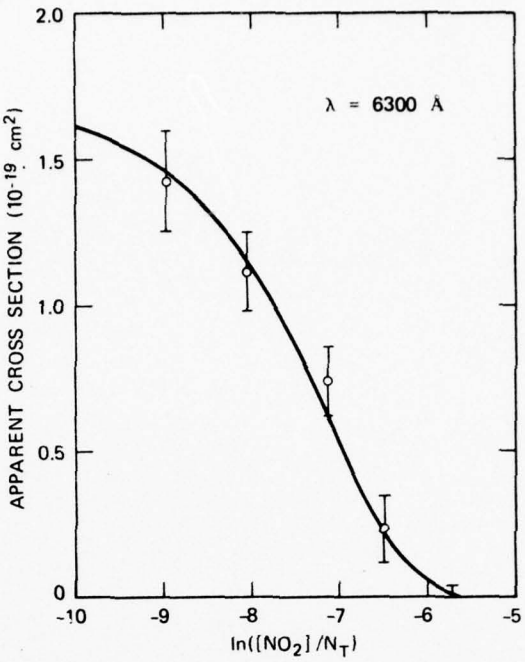

FIG. 3. Apparent photodetachment cross section of NO_2^- as a function of the relative NO_2 pressure at 6300 Å. The smooth curve is calculated using the deexcitation rates given in Table I.

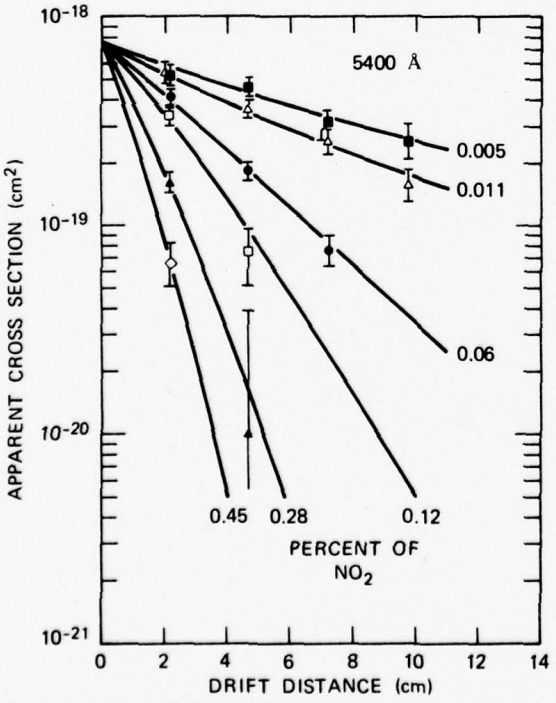

FIG. 2. Apparent photodetachment cross sections of NO_2^- for various NO_2 concentrations as a function of drift distance at a photon energy of 2.25 eV (5400 Å). The solid curves are calculated from the two level model.

E/N of 10 Td, NO_2^- is formed by the rapid charge transfer reactions:

$$O^- + NO_2 \xrightarrow{k_1} NO_2^- + O, \tag{2a}$$

$$O_2^- + NO_2 \xrightarrow{k_2} NO_2^- + O_2, \tag{2b}$$

with reported[12-14] rate constants $k_1 \cong k_2 = 1.2\times10^{-9}$ cm^3/sec. The apparent photodetachment cross section σ of this NO_2^- is found to vary markedly with drift distance and total gas pressure as well as with the relative NO_2 concentration. Figures 1 and 2 show the strong decrease of σ with increasing drift distance for various NO_2 concentrations in O_2 at two photon energies. This cross section also decreases as the total pressure is increased, with the other parameters fixed, indicating the important role of the number of collisions the NO_2^- ions undergo before the interaction with the laser beam. The decrease of the apparent photodetachment cross section is faster at longer photon wavelengths. Figure 3 shows the variation of σ with the NO_2 concentration. At a fixed drift distance of 4.3 cm the apparent cross section drops rapidly from 1.4×10^{-19} cm^2 to below 4×10^{-21} cm^2 as the relative NO_2 concentration is increased from 0.013% to 0.32%. At higher concentrations of NO_2 or at longer drift distances, the value of the apparent photodetachment cross section is found to approach zero. Similar dependences on both of the parameters have been measured at 5400 Å. Thus, the apparent photodetachment threshold of NO_2^- can be varied over a range of at least 0.3 eV by a suitable choice of drift tube conditions. Measurements in the other two gas mixtures showed the same qualitative features.

In an attempt to characterize these observations quantitatively, we have developed a simple model of the reaction kinetics in which the NO_2^- is treated as a two-level system having one excited level which photodetaches and a ground level which does not. This model seems logical as a first approximation, and should be reliable if the excited state is electronically or structurally different from the ground state. However, it is certainly oversimplified if the excitation is vibrational. It is important to note that the measured photodetachment cross section of NO_2^- as a function of NO_2 concentration and drift distance is used simply to monitor the number of remaining excited NO_2^- ions at the exit to the drift tube.

Due to exothermicity of reactions (2) and the different bond angles of NO_2 and NO_2^-, we assume that all of the NO_2^- ions are formed in the excited level. The effect of cases where the NO_2^- is only partially excited, and where the excitation involves a number of levels will be discussed below. The NO_2^- ions formed along the drift length are assumed to be partially deexcited by collisions with the neutral gas before they interact with the laser beam. Taking the position of formation of NO_2^- and its deexcitation by NO_2 and O_2 explicitly into account, we are able to account satisfactorily for the observed variations of the apparent cross section with drift distance and gas composition.

The total number of NO_2^- ions and the number of excited NO_2^{-*} passing a plane at a drift distance d per second are given by

$$(NO_2^-)_d = (O^-)_0(1 - e^{-\alpha_1 d}) + (O_2^-)_0(1 - e^{-\alpha_2 d}) \tag{3}$$

and

$$(NO_2^{-*})_d = (O^-)_0 \cdot \frac{\alpha_1}{\beta - \alpha_1} \cdot (e^{-\alpha_1 d} - e^{-\beta d}) + (O_2^-)_0 \cdot \frac{\alpha_2}{\beta - \alpha_2} (e^{-\alpha_2 d} - e^{-\beta d}), \tag{4}$$

where

$$\alpha_1 = [NO_2] \cdot k_1 / v_D(O^-), \tag{5}$$

$$\alpha_2 = [NO_2] \cdot k_2 / v_D(O_2^-), \tag{6}$$

and

$$\beta = N_T \cdot k_{DE} / v_D(NO_2^-). \tag{7}$$

The following definitions are used: $[NO_2]$ is the density of NO_2 gas; N_T is the total gas density; $(O^-)_0$ and $(O_2^-)_0$ are the numbers of O^- and O_2^- ions passing zero drift distance per second; k_{DE} is the total deexcitation rate; and $v_D(X^-)$ is the ion drift velocity of X^-. We note that the relative density profiles of all the ions in the swarm are the same at any given drift distance, since the ratio of the spread of an ion cloud to the drift distance is independent of the diffusion coefficient and mobility at low E/N.[15] Thus, diffusion need not be considered in this analysis.

The decrease of the observed NO_2^- signal due to the interaction with the laser is given by

$$\Delta(NO_2^{-*}) = f \cdot (NO_2^{-*})_d \cdot (1 - e^{-\sigma_0 \cdot \varphi \cdot \tau / \kappa}), \tag{8}$$

where

σ_0 = photodetachment cross section for the excited NO_2^{-*};

φ = photon flux;

τ = interaction time (drift time through laser beam);

κ = geometric factor describing the overlap of the laser and the observed portion of the ion swarm; and

f = the fraction of NO_2^{-*} and NO_2^- ions observed by the detection system.

From (3), (4), and (8) we obtain the following expression for the ratio of the NO_2^- counting rates for the laser on and off:

$$\frac{I}{I_0} = \frac{f \cdot (NO_2^-)_d - \Delta(NO_2^{-*})}{f \cdot (NO_2^-)_d} = \left[1 - (1 - e^{-\sigma_0 \varphi \tau / \kappa}) \cdot \left((O^-)_0 \frac{\alpha_1}{\beta - \alpha_1}(e^{-\alpha_1 d} - e^{-\beta d}) + (O_2^-)_0 \frac{\alpha_2}{\beta - \alpha_2}(e^{-\alpha_2 d} - e^{-\beta d}) \right) \cdot [(O^-)_0(1 - e^{-\alpha_1 d}) + (O_2^-)_0(1 - e^{-\alpha_2 d})]^{-1} \right]. \tag{9}$$

Note that since the density profiles of NO_2^- and NO_2^{-*} are the same and no mass discrimination between the two ions is likely to occur, the factor f in Eq. (9) is equal to that in Eq. (8).

Using the following expression[10] for the apparent photodetachment cross section

$$\sigma = \frac{\kappa}{\varphi \tau} \ln(I_0/I), \tag{10}$$

we obtain

$$\sigma = -\frac{\kappa}{\varphi \tau} \ln \left[1 - \left((O^-)_0 \frac{\alpha_1}{\beta - \alpha_1}(e^{-\alpha_1 d} - e^{-\beta d}) + (O_2^-)_0 \frac{\alpha_2}{\beta - \alpha_2}(e^{-\alpha_2 d} - e^{-\beta d}) \right) (1 - e^{-\sigma_0 \varphi \tau / \kappa}) \cdot [(O^-)_0(1 - e^{-\alpha_1 d}) + (O_2^-)_0(1 - e^{-\alpha_2 d})]^{-1} \right]. \tag{11}$$

For the limiting cases $d = 0$ or $k_{DE} = 0$ ($\beta = 0$) this expression reduces to $\sigma = \sigma_0$, as expected, assuming all the ions are initially formed in the excited state. Otherwise, σ is only a lower limit for σ_0 at $d = 0$. However, σ_0 also represents the photodetachment cross section for NO_2^- in whatever initial distribution of states it is formed, whether or not the two level model is valid.

All of the quantities in Eq. (11) are known or measured except k_{DE} (in β) and σ_0. These quantities were varied in Eq. (11) to fit the experimental data. The resulting fits are shown as the solid lines in Figs. 1 and 2, where σ_0 is the $d = 0$ intercept. The values of k_{DE} are shown in Fig. 4 as a function of the NO_2 concentration. Clearly, NO_2^{-*} is deexcited at substantially different rates by O_2 and NO_2. Assuming two different deexcitation rates $k_{DE}(O_2)$ and $k_{DE}(NO_2)$ for collisions with O_2 and NO_2, the following relation should be fulfilled:

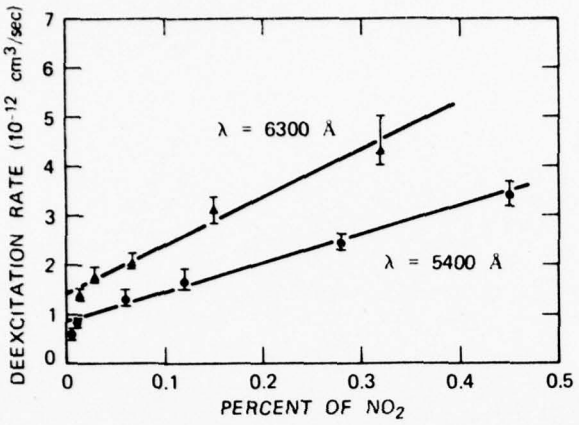

FIG. 4. Variation of the total deexcitation rate with NO_2 concentration for two different photon energies.

$$k_{DE} \cdot N_T = k_{DE}(O_2) \cdot [O_2] + k_{DE}(NO_2) \cdot [NO_2]. \quad (12)$$

For the small amounts of NO_2 used here we have

$$k_{DE} \cong k_{DE}(O_2) + k_{DE}(NO_2) \cdot [NO_2]/N_T. \quad (13)$$

The values for the different deexcitation rates calculated from (13) are given in Table I.

These rates, of course, are only approximations to the actual deexcitation rate of a single excited level in NO_2^-. Our use of a two-level model does not imply that we believe only two levels of these ions are involved in this process, but it is the simplest model which could represent the experimental data at a single wavelength. In fact, the increase of the deexcitation rates and the decrease of σ_0 with increasing wavelength shows that the NO_2^- is not a two level system, which would result in a constant rate and σ_0.

IV. DISCUSSION OF UNCERTAINTIES

The uncertainties in the measured photodetachment cross sections, such as those shown in Figs. 1–3, arise primarily from the statistical uncertainty in $\ln(I_0/I)$ in Eq. (10). This uncertainty has been extensively discussed in earlier publications.[10,11]

The uncertainties in the deexcitation rates arise primarily from the uncertainty in the relative amounts of $(O^-)_0$ and $(O_2^-)_0$, their respective rates for the formation of NO_2^-, k_1 and k_2, and the partial pressure of NO_2. The deexcitation cross sections were determined using the relative concentrations of O^- and O_2^- calculated from their measured count rates at short drift distance. For all the reported experiments their concentration were nearly equal. The error bars in Fig. 4 represent the maximum uncertainty possible from this effect if the NO_2^- ions are formed entirely from O^- (upper limit) or from O_2^- (lower limit). In fact, the uncertainty from this effect is probably negligible. The uncertainty in the k_{DE} due to the uncertainties in k_1 and k_2 can be similarly assessed. Assuming both rates may be in error by ± 25%, the same error bars in Fig. 4 are obtained. The upper limit is for the case where both rates are low by 25%; the lower limit where both rates are high by 25%. The uncertainty in the NO_2 partial pressure of ± 30% leads to a ±25% uncertainty in the deexcitation rates. Thus, in the worst case the reported rates could be in error by 50%; the most probable range of uncertainty is ± 30%.

The uncertainty in σ_0 is smaller, due to the large amount of data obtained and the reasonable extrapolation procedure used. We assign an absolute uncertainty of ± 20%, which includes the uncertainty induced by the normalization to O_2^- to obtain absolute cross section values.

V. IDENTITY OF THE NO_2^- EXCITED STATES

It remains to identify the excited states of NO_2^- whose photodetachment is observed. Three possibilities have been previously suggested[5]: the metastable $NO_2^-(^3B_1)$ state, the postulated peroxy (NOO^-) isomer, and excited vibrational levels of the ground $NO_2^-(X\,^1A_1)$ state.

The lowest triplet state of $NO_2^-(^3B_1)$ has been calculated to lie 1.7[16] and 2.35[17] eV above the ground $X\,^1A_1$ state. The charge exchange reaction (2a) with O^- to form NO_2^-, which is only 1 eV exothermic, would not be expected to produce $NO_2^-(^3B_1)$. From reaction (2b) with O_2^-, which is 1.9 eV exothermic, formation of NO_2^- in the $^3B_1$ state might be energetically possible. However, when the ratio $[O^-]/[O_2^-]$, produced in the source was varied from 0.47 to 1.12 at 6300 Å, no significant change was observed in the apparent photodetachment cross section, indicating that the excited NO_2^- species is formed with comparable efficiencies from both O^- and O_2^-. Further, it seems unlikely that such an excited state would survive several hundred collisions with O_2, as does the observed excited species.

The postulated isomer of NO_2^- would certainly exhibit a lower energy photodetachment threshold, and would probably undergo rapid charge exchange with NO_2, resulting in the observed rapid deexcitation by NO_2. However, it is difficult to explain the deexcitation of this isomer by thermal energy collisions with O_2, even if the expected energy barrier is substantially less than 1.2 eV. It is also difficult to explain the formation of this isomer. Under our experimental conditions, the observed NO_2^- must be formed primarily from O^- and O_2^- at near thermal energies. Reactions (2a) and (2b) are not sufficiently exothermic to produce

TABLE I. Deexcitation rates and photodetachment cross section for NO_2^-*.

λ(A)	5400	5500	6300
σ_0 (cm^2)	7.5×10^{-19}	6.7×10^{-19}	4.8×10^{-19}
$k_{DE}(O_2)\left(\frac{cm^3}{sec}\right)$	8.5×10^{-13}		1.4×10^{-12}
$k_{DE}(NO_2)\left(\frac{cm^3}{sec}\right)$	5.9×10^{-10}		9.7×10^{-10}
$k_{DE}(CO_2)\left(\frac{cm^3}{sec}\right)$		10^{-11}–10^{-12}	

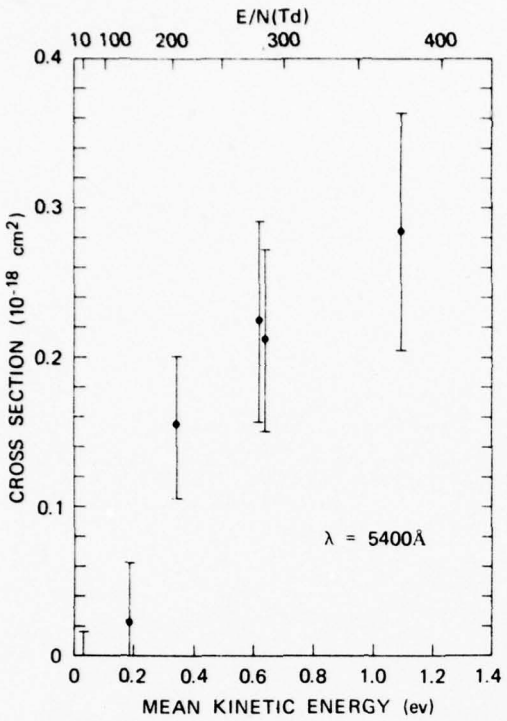

FIG. 5. Apparent photodetachment cross section of NO_2^- as a function of the ion mean kinetic energy.

the isomeric form, and we do not observe other reactions forming the NO_2^-. The photodetachment of a mixture of isomeric and normal NO_2^- would also probably follow our two level model and the deexcitation rates would be independent of wavelength, contrary to observation.

Consider now what would be expected in the photodetachment of highly excited vibrational levels of the ground $X\,^1A_1$ state. Clearly this would not be a two level system, and the higher vibrational levels should be depopulated faster than lower ones, since the higher levels could populate lower ones upon relaxation. Thus the apparent deexcitation rate should increase with increasing wavelength, since longer wavelengths would sample only higher vibrational levels. This behavior is consistent with the experimental observation (see Table I). Furthermore, the apparent "zero-collision" cross section σ_0 would be expected to decrease with increasing wavelength, qualitatively because fewer vibrational levels can be detached at longer wavelengths. This has been shown quantitatively by calculations[5] that include the appropriate vibrational overlap integrals. Again, the expected behavior is consistent with our observations (see Table I).

A corollary to the decrease of σ_0 with wavelength is that the apparent photodetachment cross section σ would be expected to increase with increasing vibrational excitation. This effect was investigated by using a drift field with two regions of different E/N. The ions leaving the source first drift for 20 cm at E/N of 10 Td in O_2 with 0.3% NO_2. This low E/N drift region guarantees essentially relaxed ions and "zero" photodetachment cross section at the end of this 20 cm (see Figs. 1 and 2). In the following 20 cm just preceding the laser interaction region, E/N was varied up to 400 Td, yielding an apparent photodetachment cross section at 5400 Å shown in Fig. 5. Increasing E/N increases the mean collision energy of the ions, and therefore will result in increased vibrational excitation. The mean kinetic energy as calculated from the Wannier relation[18] is also shown in Fig. 5. The increase of the photodetachment cross section with increasing E/N is consistent with collisional excitation of vibrational levels. We would not expect to produce isomeric NO_2^- nor to populate the $^3B_1$ state at these low collision energies.

We observe a de-excitation rate for NO_2^- by O_2 of about 10^{-12} cm^3/sec, and a slightly larger rate by CO_2. Observed rates for the vibrational de-excitation of neutral triatomics in various gases[19–21] range from 10^{-11} to 10^{-14} cm^3/sec. NO_2 would be expected to have a substantially larger deexcitation rate for NO_2^- due to resonant charge transfer and more efficient transfer of vibrational energy between the ion and its parent molecule.

Finally, formation of NO_2^- by the charge exchange reactions (2a) and (2b) would be expected to result in substantial vibrational excitation due to the significantly different bond angle and length in the neutral and the ion,[5] and the exothermicity of the charge exchange reactions (approximately 1 and 1.9 eV, respectively). Neither of these reactions, however, is sufficiently exothermic to efficiently populate the $^3B_1$ state (1.7–2.35 eV), nor to reach the peroxy isomer[9] (3.2 eV).

All of our observations are therefore consistent with the formation, deexcitation, and photodetachment of vibrationally excited $X\,^1A_1\,NO_2^-$, and some of our observations are difficult to explain if the excited state is assumed to be either the $^3B_1$ or the peroxy isomer.

VI. COMPARISON WITH PREVIOUS RESEARCH

Adams, Bohme, Dunkin, Fehsenfeld, and Ferguson[7] studied reaction (1) in a flowing afterglow, and determined an equilibrium constant of 11. The forward rate constant had previously been measured[22] to be 9×10^{-12} cm^3/sec. Since the reaction is strongly exothermic in the forward direction, Adams *et al.* concluded that the NO_2^- formed in reaction (1) must be excited and must maintain a significant part of this excitation through ~300 collisions with the background O_2 gas in order to yield the equilibrium constant of 11. They considered vibrational excitation as the most likely form of excitation, but suggested the possibility of both electronic excitation and an isomeric state.

Using the equilibrium constant of 11, the reverse reaction rate is 8×10^{-13} cm^3/sec, approximately equal to our measured deexcitation rate for NO_2^- in O_2. Thus, the reported reaction rate and equilibrium constant are consistent with our measured de-excitation rate. We also briefly studied the deexcitation of NO_2^- formed in CO_2 with a trace of NO, presumably by reaction (1). The observed deexcitation rate by CO_2 was somewhat larger

than that by O_2, but the presence of small but unknown quantities of NO_2 could have contributed significantly to this deexcitation, and to the formation of some NO_2^- by reactions (2). The deexcitation of NO_2^- by CO_2 might be expected to be somewhat faster than by O_2 due to the additional degrees of freedom and larger size of the molecule. It thus appears that the amount of excitation in NO_2^- formed by reaction (1) and that formed in reactions (2a) and (2b) is comparable, and all three reactions probably lead to vibrational excitation of the ground state.

Richardson, Stephenson, and Brauman[8] investigated the photodetachment of NO_2^- using ion cyclotron resonance techniques. They observed a long wavelength tail below the ground state threshold which was attributed to a peroxy form of NO_2^-. Considering our measured deexcitation rate of NO_2^- by NO_2, it appears likely that a substantial fraction of any vibrationally excited NO_2^- produced in their source could survive the trapping times in the ICR spectrometer.[23] The NO_2^- in this experiment was reported to be produced by direct electron attachment at 1.5 to 2.4 eV rather than reactions (1) or (2), but again because of the different bond angles and lengths in the ion and the neutral, direct electron attachment should result in vibrationally excited NO_2^-. These low electron energies would also seem to preclude the structural changes required to form the peroxy isomer. The arguments favoring the observation of a peroxy isomer in this experiment seem now to be less compelling, although on the basis of our data alone it is not possible to say with certainty that a peroxy isomer was not observed by Richardson *et al.*

In their study[5] of the photodetachment of NO_2^-, Herbst, Patterson, and Lineberger observed an onset in the photodetachment at about 1.8 eV when the NO_2^- was produced in a discharge source filled with O_2 and a trace amount of N_2. When the NO_2^- was formed in pure NO_2 the onset in the photodetachment was near 2.2 eV. They attributed the lower energy onset to an isomeric form of NO_2^-. The present determination that the deexcitation of vibrationally excited NO_2^- is 2 to 3 orders of magnitude faster by NO_2 than by O_2 provides a reasonable explanation for their results without invoking an isomeric state. If some of the NO_2^- is in an isomeric state, one should observe an invariant threshold near 1.8 eV, independent of source conditions. It would therefore be informative to study the photodetachment of NO_2^- in their apparatus using O_2 with varying small amounts of NO_2 in the source. Our results would predict that the apparent threshold should vary smoothly from 1.8 to 2.2 eV as the NO_2 concentration was increased.

VII. CONCLUSIONS

We have observed the photodetachment of excited NO_2^- at photon energies below the threshold for photodetachment of the ground vibrational level. Deexcitation rates for this NO_2^-* by O_2, NO_2, and CO_2 have been measured, and "zero-collision" photodetachment cross sections determined for NO_2^-* formed by reactions (2). The experimental results are consistent with the expectation that the NO_2^- is formed vibrationally excited. Using our measured deexcitation rates, it is reasonable to attribute earlier observations[5,8] of excited NO_2^- to vibrational excitation. Photoelectron spectroscopy[24] of the excited NO_2^- might resolve this issue.

In the ionosphere, NO_2^- is principally destroyed by reaction with O_3 and by photodetachment. The total rate of destruction[1] by both these channels for ground state NO_2^- is much less than 1 sec^{-1}. Assuming a mean rate constant of 5×10^{-13} cm^3/sec for NO_2^-* the collisional deexcitation rate for NO_2^-*in the *D*-region of the ionosphere is ~5000 sec^{-1}. Thus, if the total rate of destruction of excited NO_2^- by reactions and photodetachment is a factor of 10^3 greater than that of ground state NO_2^-, the effect of this excitation in the ionosphere could be important. An estimation of the sunlight photodetachment rate of excited NO_2^-, based on our three measured values of σ_0, indicates that it is unlikely to be more than 10 times greater than that for ground state NO_2^-. Ion–molecule reaction rates of excited NO_2^- have not been measured, but it seems unlikely that they will exceed those of the ground state by more than a factor of 10. We therefore tentatively conclude that the effect of this excitation produced in NO_2^- when it is formed should be negligible in the ionosphere.

This study demonstrates a new technique for the investigation of collisional deexcitation processes, namely, the use of photodestruction processes to monitor the amount of excitation of a molecular species. Ion–molecule reaction rates involving excited ionic species can also be measured using the laser to monitor the excited ions. It has been suggested[23] that by measuring the photodetachment cross section as a function of wavelength for a wide range of the degree of excitation of the NO_2^-, and then fitting these cross sections using appropriate Franck–Condon factors[5] one could in principle obtain the populations of the individual vibrational levels for each degree of excitation. In this way one could obtain deexcitation rates for the individual vibrational levels, rather than an overall effective rate as determined here.

ACKNOWLEDGMENTS

We would like to acknowledge valuable discussions with Professor John Brauman and his students and with Professor Carl Lineberger concerning the interpretation of our results. B.A.H. acknowledges the support of the Deutsche Forschungsgemeinschaft for his participation in this research.

*This research was supported by the U. S. Army Ballistics Research Laboratories through the U. S. Army Research Office.

†Permanent address: Ruhruniversität, Institut für Experimentalphysik II, 463 Bochum, West Germany.

[1]L. Thomas, Radio Sci. **9**, 121 (1974); and references therein.

[2]D. B. Dunkin, F. C. Fehsenfeld, and E. E. Ferguson, Chem. Phys. Lett. **15**, 257 (1972).

[3]B. M. Hughes, C. Lifshitz, and T. O. Tiernan, J. Chem. Phys. **59**, 3162 (1973).

[4]S. T. Nalley, R. N. Compton, H. C. Schweinler, and V. E.

Anderson, J. Chem. Phys. **59**, 4125 (1973).
[5]E. Herbst, T. A. Patterson, and W. C. Lineberger, J. Chem. Phys. **61**, 1300 (1974).
[6]*Defense Nuclear Agency Reaction Rate Handbook* (DNA 1948H), edited by M. H. Bortner and T. Bauer (DASIAC, G. E. Tempo, Santa Barbara, CA, 1972), p. 17-11.
[7]N. G. Adams, D. K. Bohme, D. B. Dunkin, F. C. Fehsenfeld, and E. E. Ferguson, J. Chem. Phys. **52**, 3133 (1970).
[8]J. H. Richardson, L. M. Stephenson, and J. I. Brauman, Chem. Phys. Lett. **25**, 318 (1974).
[9]P. K. Pearson, H. F. Schaefer, T. H. Richardson, L. M. Stephenson, and J. I. Brauman, J. Am. Chem. Soc. **96**, 6778 (1974).
[10]J. T. Moseley, P. C. Cosby, R. A. Bennett, and J. R. Peterson, J. Chem. Phys. **62**, 4826 (1975); P. C. Cosby and J. T. Moseley, Phys. Rev. Lett. **34**, 1603 (1975).
[11]P. C. Cosby, R. A. Bennett, J. R. Peterson, and J. T. Moseley, J. Chem. Phys. **63**, 1612 (1975); P. C. Cosby, J. H. Ling, J. R. Peterson, and J. T. Moseley, *ibid* (in press).
[12]E. E. Ferguson, Can. J. Chem. **47**, 1815 (1969).
[13]C. Lifshitz and R. Tassa, Int. J. Mass. Spectrosc. Ion. Phys. **12**, 433 (1973).
[14]F. C. Fehsenfeld and E. E. Ferguson, J. Chem. Phys. **61**, 3181 (1974).
[15]E. W. McDaniel, *Collision Phenomena in Ionized Gases* (Wiley, New York, 1964), p. 494.
[16]W. England, P. Fortune, D. Hopper, B. Rosenberg, G. Das, and A. C. Wahl, Abstracts, 30th Symp. on Mol. Struc. and Spec., Ohio State University, 1975, p. 83.
[17]R. M. Hochstrasser and A. P. Marchetti, J. Chem. Phys. **50**, 1727 (1969).
[18]Reference 15, p. 438.
[19]C. W. van Rosenberg and D. W. Trainor, J. Chem. Phys. **61**, 2442 (1974).
[20]D. I. Rosen, T. A. Cool, J. Chem. Phys. **54**, 6097 (1973); **62**, 466 (1974).
[21]R. T. V. Kung, J. Chem. Phys. **63**, 5305, 5313 (1975).
[22]E. E. Ferguson, Can. J. Chem. **47**, 1815 (1969).
[23]J. I. Brauman, Stanford University (private communication).
[24]M. W. Siegel, R. J. Celotta, J. L. Hall, J. Levine, and R. A. Bennett, Phys. Rev. A **6**, 607 (1972).

APPENDIX C

PHOTON INTERACTIONS INVOLVING NO_2^-, NO_3^-, AND THEIR HYDRATES*

P. C. COSBY, G. P. SMITH, J. R. PETERSON, and J. T. MOSELEY

Molecular Physics Center, Stanford Research Institute,
Menlo Park, California 94025

Photodestruction of the ions NO_2^-, $NO_2^- \cdot D_2O$, NO_3^-, and $NO_3^- \cdot D_2O$ has been investigated using a drift tube mass spectrometer-dye laser apparatus[1] at wavelengths between 6300 and 5150 Å.

The NO_2^- and NO_3^- ions, formed in a 1:20 NO/O_2 mixture at 0.5 torr, drift fields of 0.5-1.0 x 10^{-16} V-cm^2, and drift distances of 7.6-25 cm, are found to have no measurable photodestruction cross section (< 3 x 10^{-20} cm^2). However, when NO_3^- is prepared in N_2O gas containing a trace of O_2, at a total pressure of 0.15-1.0 torr, the photodissociation reaction

$$NO_3^- + h\nu \rightarrow O_2^- + NO \qquad (1)$$

is observed. The cross section for this reaction increases from 3 x 10^{-19} cm^2 at 5675 Å to 1.5 x 10^{-18} cm^2 at 5150 Å and is independent of photon flux, total pressure, and drift distance. Since the lowest energy dissociation channel for ground state NO_3^- is 4.3 eV[2], the species produced in the N_2O mixture is believed to be the peroxy isomer $O_2^- \cdot NO$. It has been previously postulated[3] that this isomer is formed in the reactions of $O_2^- \cdot H_2O$, O_4^-, and CO_4^- with NO gas, and rapidly undergoes the reaction[3]

$$O_2^- \cdot NO + NO \rightarrow NO_2^- + NO_2 \quad , \qquad (2)$$

whereas ground state NO_3^- does not. In the NO/O_2 mixture, given the rates for the formation of $O_2^- \cdot NO$ and its rate of destruction via reaction (2), only trace amounts of this species would be present in the photon beam, while ground state NO_3^-, formed from NO_2 impurities in the NO gas, would be present in far greater abundance.

The $NO_2^- \cdot D_2O$ and $NO_3^- \cdot D_2O$ ions are produced by the addition of approximately 5 x 10^{-4} torr of D_2O to either the O_2/N_2O or NO/O_2 mixtures. The cross section for photodestruction of $NO_2^- \cdot D_2O$ is less than 4 x 10^{-20} cm^2, and possibly zero. Photodestruction of $NO_3^- \cdot D_2O$, however, is observed with a cross section which varies from 3 x 10^{-19} cm^2 at 5300 Å to 6 x 10^{-19} cm^2 at 5150 Å. Moreover, the cross section for this ion is independent of which of the two gas mixtures is used for its production. We believe this ion which undergoes photodestruction is actually the hydrate of $O_2^- \cdot NO$ rather than that of ground state NO_3^-. In the O_2/N_2O mixture, the hydrate would be formed from the three-body association of $O_2^- \cdot NO$ with

D_2O, while in NO/O_2 the reaction[3]

$$O_2^-\cdot(D_2O)_2 + NO \rightarrow O_2^-\cdot NO\cdot D_2O + D_2O \qquad (3)$$

is probably responsible for $O_2^-\cdot NO\cdot D_2O$ production. The apparent stability of $O_2^-\cdot NO\cdot D_2O$ with respect to reaction with NO could be significant in the evaluation of negative ion reaction schemes in the lower ionosphere.

When the ions $NO_2^-\cdot D_2O$ and $NO_3^-\cdot D_2O$ are produced in NO_2/Ar or NO_2/O_2 mixtures, destruction of these ions when the photon beam is on is observed with a corresponding appearance of NO_2^- and NO_3^- products. However, the apparent cross section for an assumed photodissociation process varies markedly with NO_2 total pressure, and approaches zero in the limit of zero NO_2 concentration. Moreover, the wavelength dependence of the apparent cross section closely follows that of the NO_2 total absorption cross section[4] in this wavelength region. This suggests the reactions

$$NO_2 + h\nu \rightarrow NO_2^* \qquad (4)$$

$$NO_x^-\cdot D_2O + NO_2^* \rightarrow NO_x^- + D_2O + NO_2 \qquad (x = 2,3) \qquad (5)$$

occur in the photon interaction region of the drift tube. From the magnitude of the destruction observed, the cross sections in reaction (5) for $NO_2^-\cdot D_2O$ and $NO_3^-\cdot D_2O$ are estimated to be of order 10^2 Å^2 and 10 Å^2, respectively. Destruction is also observed for the ions $NO_2^-\cdot H_2O$, $NO_2^-\cdot NO_2$, and $NO_3^-\cdot NO_2$ produced under the same conditions.

* Research supported by U.S. Army Ballistics Research Laboratory through Army Research Office.

1 P. C. Cosby, J. H. Ling, J. R. Peterson, and J. T. Moseley, J. Chem. Phys. 65, 5267 (1976).

2 F. C. Fehsenfeld, A. L. Schmeltekopf, H. I. Schiff, and E. E. Ferguson, Planet. Space Sci. 15, 373 (1967).

3 F. C. Fehsenfeld and E. E. Ferguson, J. Chem. Phys. 61, 3181 (1974); and references therein.

4 D. Hsu and R. N. Zare, private communication (1977).

APPENDIX D

PHOTODISSOCIATION SPECTROSCOPY OF O_3^{-*}

P. C. Cosby, J. T. Moseley, J. R. Peterson and J. H. Ling†
Molecular Physics Center
SRI International, Menlo Park, California 94025

ABSTRACT

The photodissociation cross section of gas-phase O_3^- has been measured using a tunable dye laser over a wavelength range of 6400-5080 Å. The cross section exhibits considerable structure, which is consistent with dissociation from vibrational levels of a quasi-bound excited electronic state. Analysis of the structure indicates progressions in two vibrational modes of the excited state. Photodissociation spectra of ions prepared in both excited and ground vibrational levels also yields two vibrational frequencies for the ground X^2B_1 state and an apparent rate coefficient for vibrational relaxation in O_2. The molecular constants determined here for the two O_3^- electronic states are compared with those obtained from absorption spectra of the ion in other media. Identification of the dissociating state is discussed.

†Present address: 10756 Bartlett Ave., NE, Seattle, Washington

MP 77-93

I. Introduction

The O_3^- ion is an important intermediate in current D-region negative ion reaction schemes of the ionosphere.[1] This ion also represents a relatively simple triatomic system for which detailed calculations[2-5] of its electronic structure are becoming feasible. The O_3^- ion has been studied in ozonide[6] and chlorate[7,8] crystals, in liquid ammonia solution,[6,9,10] and isolated in rare gas matrices.[11-15] From these resonance raman, infrared, and visible absorption spectra a number of molecular constants have been measured for the ion in these environments.

The formation and reactions of O_3^- in the gas phase have been studied by a number of investigators using drift tube,[16,17] flowing afterglow,[18,19] and beam[20-23] techniques. The photodetachment cross section of this ion has been measured[24] and the electron affinity of O_3 obtained both from these data and from ion-molecule reaction[19,21-23] studies. We have previously reported[25,26] the total photodestruction cross section of O_3^- between 6400-4579 Å and have observed photodissociation of the ion in this wavelength region. It was suggested there that the structure in the cross section reflected absorption into levels of an excited electronic state of O_3^- which is predissociated. The purpose of the present paper is to present an analysis of the O_3^- photodestruction cross section and to attempt to characterize the states of O_3^- relevant to the dissociation process.

II. Experimental

The experiments were performed using a drift tube mass spectrometer-tunable dye laser apparatus, which has been previously[27] described. O^- ions are produced in the ion source by dissociative electron attachment[28] of O_2. These ions enter the drift region, which contains O_2 at a pressure of 0.3-0.4 torr, and move down the drift tube under the influence of a weak, applied electric field. The ratio of the electric field strength to O_2 gas density (E/N) was maintained at 5 Td (1 Td = 10^{-17} V-cm^2) so that the directed drift velocity was less than one-tenth the mean thermal speed of the ions and molecules at 300 K. While drifting, the O^- ions produce O_3^- by the three-body reaction[16,17]

$$O^- + 2O_2 \rightarrow O_3^- + O_2 \quad . \tag{1}$$

The drift region is terminated by an end plate containing a 1-mm diameter extraction aperture. Ions passing through this aperture enter a high vacuum region where they are mass selected by a quadrupole mass spectrometer and detected individually by an electron multiplier.

Just prior to entering the extraction aperture the ion swarm intersects the cavity of the tunable dye laser. The photon beam has a diameter of approximately 2 mm and its axis is positioned within 2 mm of the extraction aperture. The total photodestruction cross section of an ion is measured by chopping the laser at 100 Hz, tuning the mass spectrometer to the appropriate mass, and counting the number of ions arriving at the detector during the alternate periods when the laser is on and off. Photofragment ions resulting from a photodissociation can also be identified.

The distance from the ion source to the laser interaction region can be varied over a range of 2.5-50.8 cm. Thus both the ratio of O_3^-/O^- ions arriving at the laser and the number of "thermalizing" collisions the ions undergo prior to photon interaction can be varied over a wide range.

The dye laser used in this experiment is a commercial "jet-stream" model pumped by a 16 W argon ion laser. The laser had a linewidth of approximately 0.4 Å (FWHM) and its wavelength was set relative to a calibrated monochromator to a precision of 0.5 Å and an absolute accuracy of $\pm$ 1 Å.

All reported cross sections were measured relative to the O^- photodetachment data of Branscomb, Smith, and Tisone.[29] However, photodissociation of O_3^- to produce O^- occurs[26] in the wavelength range reported here. In order to avoid the error[25] introduced into the apparent O^- photodetachment cross section by the photofragment O^- ions, the O_3^- cross section is measured relative to the O_2^- photodetachment cross section. The cross section for O_2^- has been measured[26] at lower pressures, in the absence of O_3^-, relative to that of O^-. At photon energies less than approximately 2.1 eV, the production of photofragment O^- becomes immeasurably small and identical O_3^- photodestruction cross sections are obtained relative to either the O^- or O_2^- cross sections.

III. Photodissociation Spectrum

The total photodestruction cross section of O_3^- is shown in Fig. 1 as a function of photon energy. These data were obtained at a drift distance of 30.5 cm in 0.3 torr of O_2 gas. The absolute error in the cross section scale is $\pm$ 12% which includes the uncertainties in the O^- and O_2^- cross sections and in the relative mobilities[30] of O_2^- and O_3^-. The error bars in this figure are the statistical (counting) errors for O_2^- and O_3^- at each photon energy. An additional source[31] of error must be considered for the data at photon energies less than about 2.08 eV. Since a small quantity of unreacted O^- ions is present in the laser interaction region, the destruction of a fraction of these ions by photodetachment will produce a loss of these O_3^- ions, which would have been produced in this region by reaction (1) had the O^- ions not been photodetached. The effect of this small loss becomes increasingly significant as the O_3^- photodestruction cross section decreases. At the lowest photon energy shown, this O^- loss is equivalent to an apparent O_3^- photodestruction cross section of 1.6×10^{-20} cm^2. The photodestruction cross section has been corrected for this effect and the error bars in Fig. 1 reflect the uncertainties in the correction procedure.

The O_3^- photodestruction cross section was measured at a number of laser powers ranging from 10-150 W. In this range, the data of Fig. 1 were independent of photon flux, thus establishing that the photodestruction process occurs by single photon absorptions. Two photodestruction

processes are energetically possible for ground state O_3^- ions at photon energies above 1.9 eV:

$$O_3^- + h\nu \rightarrow O^- + O_2 \quad . \tag{2}$$

and

$$O_3^- + h\nu \rightarrow O_3 + e^- \quad . \tag{3}$$

We observe photofragment O^- ions in sufficient quantities to account for $85 \pm 15\%$ of the O_3^- photodestruction at photon energies above 2.1 eV. Thus reaction (2) dominates the photodestruction spectrum at photon energies greater than this value. Below 2.1 eV the total photodestruction cross section becomes sufficiently small that the detection of photofragment O^- is difficult because changes in the O^- current are dominated by either the loss of source produced O^- through photodetachment, or by the production of photofragment O^- from trace quantities of CO_3^- ions. However, Wong, Vorburger, and Woo[24] have reported a cross section for reaction (3) which varies smoothly from $3.1 \pm 3.2 \times 10^{-19}$ cm^2 to $5.3 \pm 2.6 \times 10^{-19}$ cm^2 at photon energies between 2.0 and 2.4 eV. Consequently, the contribution of reaction (3) to the total destruction in this region is negligible and the data shown in Fig. 1 can be considered the O_3^- photodissociation spectrum.

The photodissociation cross section in Fig. 1 consists of a series of broad maxima, each of which contains three or more narrower components. In order to identify that structure due to absorptions into the dissociating state of O_3^-, and that due to the effects of vibrationally excited levels of the O_3^- ground electronic state, which may be populated in newly formed

ions, the cross section was measured at various drift distances ranging from 5 cm to 45.7 cm. At the shortest drift distance, most O_3^- ions have undergone only a few collisions prior to the photon interaction and, in fact, almost 4% of the photodissociated O_3^- ions are produced by reaction (1) within the laser interaction region. At the longest drift distance, the O_3^- ions have undergone an average of several thousand collisions and essentially no nascent ions are present in the laser interaction region. The O_3^- photodestruction cross section was found to be independent of drift distance for photon energies greater than 2.15 eV. At lower photon energies, however, a drift distance dependence was observed. Figure 2 presents these drift distance results at five wavelengths. As can be seen from this figure, the cross section becomes increasingly dependent on drift distance as the photon energy is decreased. The cross section is largest at short drift distances, where the fraction of nascent O_3^- in the photon interaction region is expected to be greatest, and decreases in an exponential manner as the number of thermalizing collisions is increased. By subtracting the asymptotic value of the cross section at each wavelength, an approximate binary "relaxation rate"[32] for the reaction

$$O_3^{-\dagger} + O_2 \rightarrow O_3^- + O_2$$

is found to be 10^{-14} cm^3 s^{-1}.

This behavior suggests that the O_3^- ions are produced in reaction (1) with a significant amount of internal energy. An analogous case for the O_3 molecule has been reported. In observing infrared emission from nascent

O_3 formed by the reaction

$$O + 2O_2 \rightarrow O_3 + O_2 \quad ,$$

von Rosenberg and Trainor[33] found that 30-50% of the 1.05 eV exothermicity of this reaction (compared with about 1.6 eV for reaction (1)) goes into vibrational modes of the O_3 molecule. Further, these modes are relaxed by O_2 with a rate coefficient[33-35] of approximately 2×10^{-14} cm^3 s^{-1}.

The wavelength dependence of the O_3^- photodestruction cross section in the region of 2 eV is given by the upper and lower curves in Fig. 3 for drift distances of 10.3 cm and 30.5 cm, respectively. It is seen that the cross section for the less relaxed O_3^- ions is larger and exhibits structure not apparent in the cross section for ions having undergone more thermalizing collisions. We therefore conclude that, in general, features at photon energies less than approximately 2.15 eV in the photodestruction spectrum of Fig. 1 are attributable to excited levels of the O_3^- ground electronic state, whereas structure appearing at higher photon energies characterizes an excited electronic state of O_3^- which dissociates.

IV. Vibrational Assignments

Recent configuration interaction calculations[2,4,5] of O_3^- predict a $^2B_1$ ground state of C_{2v} symmetry with a bond distance of 1.27-1.41 Å and bond angle of 115-116.8°. Three excited states[4,5] are found within 4 eV of the ground state. However, dipole transitions from X $^2B_1$ are allowed only to two of these states, the $^2A_1$ and $^2A_2$. Both the $^2A_1$ and $^2A_2$ are predicted[5] to have somewhat larger equilibrium bond distances than X $^2B_1$

and the equilibrium bond angles differ from that of the ground state by approximately $+10^{o}$ and -10^{o}. Thus, optical absorptions to either of these states from the ground state would be expected to produce progressions in both the symmetric stretch and bending modes of the upper state.

The visible absorption spectrum of O_3^- has been measured for various alkali metal ozonides dissolved in liquid ammonia[9,10] or isolated in rare gas matrices.[12,15] It has also been measured in irradiated single crystals of alkali metal chlorates.[8] In each case a series of partially resolved maxima are observed extending from 2.2 to 3.5 eV, which are separated by 800 to 900 cm^{-1}. These spectra have been interpreted as absorptions from the ground electronic state of O_3^- to vibrational levels of an excited O_3^- electronic state. The energy of the transition between the lowest levels of the ground and excited electronic states was dependent on the environments in which the measurements were made, but lie within the range of 2.15 to 2.25 eV.

The widths of the maxima and their energy spacings are comparable for both the absorption spectra and the photodissociation spectrum. Also, the thresholds for these spectra occur in roughly the same photon energy regions. It therefore appears reasonable that both spectra represent transitions from the $^2B_1$ ground state of O_3^- to vibrational levels in either the $^2A_1$ or $^2A_2$ excited states.

The broad maxima in the photodissociation spectrum are spaced by roughly 800 cm^{-1}, which is comparable to the energy of vibrational stretching modes of other triatomics. The smaller components of these maxima, however,

are spaced at irregular intervals of order 150 cm^{-1}, which is unusually small. The bending mode in the $^2A_2$ state[36] of the isoelectronic molecule ClO_2, for example, is 296.3 cm^{-1}. Thus, in order to assign the structure in the photodissociation spectrum to specific levels of the excited electronic state, we searched for progressions in two or more vibrational modes of this state.

Choosing one of the three major components of the first maxima, we searched for progressions in either stretching or bending modes having energies in the range of 700-1400 cm^{-1} and 200-600 cm^{-1}. Two sets of assignments were found which provided reasonable fits to the structure. One set (I) had an origin at 2.146 eV with vibrational spacings of 855 and 290 cm^{-1}. The second set (II) had an origin at 2.163 eV with vibrational spacings of 794 cm^{-1} and 282 cm^{-1}. Neither of these sets of assignments, however, could adequately explain all of the structure observed in the spectrum. A third energy spacing of 403 cm^{-1} for set II and 419 cm^{-1} for set I corresponding to transitions to the excited electronic state from an excited vibrational mode of the X $^2B_1$ state was required. This assumption of an excited bending mode of the ground state is not in disagreement with the observed position dependence of the cross section; such a level would be populated in approximately 12% of the O_3^- ions in a Boltzman distribution at the 300°K temperature of the drift tube.

An additional assignment may be made from the photodissociation cross section measured at 10 cm drift distance (Fig. 3). The structure appearing

in the region of 2.05 eV is either 790 cm^{-1} or 928 cm^{-1} below the origin of the excited electronic state, depending on which of the two sets of assignments for the state are chosen. Further, relative to this peak, a second peak appears approximately 400 cm^{-1} lower in photon energy. It is therefore likely that these two peaks represent transitions from an excited stretching mode of the $^2B_1$ state. We assume that this mode is the symmetric stretch mode ω_1'' since the magnitude of the energy more closely approximates the energy (964 cm^{-1}) of this mode[36] in ClO_2 than that of ω_3'' (1133 cm^{-1}).

The two sets of assignments are shown in Figs. 3 and 4. In these figures, the proposed transitions are labeled by pairs of integers, the first number of which represents the quantum number of the stretching mode while the second number gives the bending mode quantum number.

Both sets of assignments predict similar vibrational frequencies for the upper state and for the bending mode of the lower state. The two sets differ primarily in the choice of origin for the upper state and, consequently, in the frequency of the lower state stretching mode. Assignment set II (the lower set in Fig. 4) shows an extended progression in the upper state stretching mode for which little or no anharmonicity is observed. This is consistent with the large difference in stretching frequencies found for the two electronic states and with the small anharmonicity observed[15] in the matrix absorption spectra. Transitions originating from the first excited level of the ground state bending mode comprise a significant portion of the spectrum at low quantum numbers, but their intensities appear to

decrease with increasing photon energy. Such a behavior is important if the room temperature photodissociation spectrum is truely comparable to matrix absorption spectra obtained at temperatures of less than $22^{o}K$.

The primary disadvantage of assignment set II is that it fails to account for the two small humps at 2.096 and 2.130 eV that occur on the low energy side of the first peak in Fig. 4. Although it is possible that these features could arise from transitions out of an excited stretching mode of the ground state (Fig. 3), the population of such a level would be relatively small at 300 K and the strength of these features does not appear to change with drift tube conditions. Assignment set I fully accounts for these features as transitions from the first excited bending mode of the lower state. Further, set I assigns the most prominent feature in the region of 2.15 eV to the origin of the upper state. This set of assignments, however, requires an anharmonicity of approximately 15 cm^{-1} in the upper state stretching frequency to obtain a fit of the observed structure. Moreover, the intensities of transitions originating from the excited lower state bending mode appear to increase with increasing photon energy. In contrast to set II, neither of these characteristics of set I would appear to be consistent with the matrix absorption spectra.

The broad widths of the peaks and the limited energy range over which the photodissociation spectrum has been measured with the dye laser do not presently allow a clear distinction between the two assignment sets, nor is it certain that either of these assignments is precisely correct. It seems certain, however, that excited state vibrational frequencies near 800 and

300 cm^{-1} are required to explain the observed structure. The low quantum numbers for the transitions also limit the usefulness of isotopic substitution in verifying the assignments. The photodissociation spectrum of $^{18}O_3^-$ (18-18-18) was briefly measured over the energy range of 2.10-2.34 eV. General shifts of the broad maxima in the regions of 2.15 and 2.25 eV by 0 ± 15 cm^{-1} and -32 ± 15 cm^{-1} were observed and are consistent with either set of assignments. Unfortunately, the quantity of $^{18}O_2$ gas available was insufficient to measure the cross sections to the precision required for detecting the small shifts expected for the individual transitions in this region. Thus, in order to better determine the vibrational assignments, extension of the dye laser measurements to 2.6 eV is planned.

The two sets of values for the vibrational energies of the O_3^- ground and excited states and for the origin of the excited state which were determined from the photodissociation spectrum are summarized in Table I. The values for the excited state constants obtained from the previously mentioned visible absorption measurements are also listed, together with the ground state constants reported from infrared and resonance raman spectra. Also shown in this table are the constants for the ClO_2 molecule, which is isoelectronic with the O_3^- ion.

The most serious disagreement between the gas phase data and those of other media occurs for the ground state energy levels. It is possible that the assignment of ω_1'' could be in error, since it was not made on the basis of an extended progression. The agreement between these data could also be improved if the gas phase data were attributed to the asymmetric stretch

mode. It is unlikely, however, that our assignment of ω_2'' is significantly in error since it is supported by a number of peaks in the photodissociation spectrum. Further, this value for the bending mode is more consistent with the energy levels of ClO_2, which were also obtained from gas-phase spectra. Undoubtedly the greatest cause for disagreement among the various spectra arises from the weak bonding[13,15] between O_3^- and the cation in rare gas matrices as well as interaction with the atoms of the matrix. Such perturbations of O_3^- can be even more serious in a crystal environment.

V. Identification of the Excited State

One important characteristic of the O_3^- photodissociation spectrum is that dissociation of the upper electronic state takes place from the lowest energy levels of that state and continues to occur over a photon energy range of at least 0.55 eV. Secondly, the degree of diffuseness in the spectral features does not noticeably vary with the vibrational level of the upper state. This also appears to be true of the absorption spectrum[15] over a photon energy range of 1.3 eV. A third characteristic is that no evidence is found for absorption into the asymmetric stretch mode of the upper state. Finally, it appears that nearly every absorption into the excited state results in a dissociation. For example, a molar extinction coefficient of 2050 L M^{-1} cm^{-1} at 4579 Å has been reported[10] for KO_3 dissolved in liquid NH_3. This coefficient, which is equivalent to an absorption cross section of 3.4×10^{-18} cm^2, compares favorably to the O_3^- photodissociation cross section of 4.9×10^{-18} cm^2 at this wavelength.

In fact, agreement between these measurements is likely to be much closer when one considers that the absorption and photodissociation cross sections are are rapidly varying functions of wavelength in this region and that the NH_3 solution absorption spectrum is shifted $\sim$ 100 Å to the blue of the gas phase photodissociation spectrum.

All these characteristics seem to indicate that a direct dissociation process, such as that recently proposed by Pack,[37] is occurring in the upper electronic state. In Pack's treatment, the potential surface of the dissociating state is considered bound along its symmetric stretch and bending coordinates, but simply dissociative along the asymmetric stretch coordinate. For vertical transitions from the bound ground state, the dissociation (absorption) cross section is proportional to products of the Franck-Condon factors for the bound wavefunctions of the symmetric stretch and bending modes of the lower and upper states, and the bound and continuum wavefunctions of the asymmetric stretch modes in these states. Thus, in contrast to the continuous spectrum previously expected[36] for direct dissociation from such a surface, the wavelength dependence of the dissociation cross section will exhibit broad peaks at wavelengths corresponding to absorption into the bound (symmetric stretch and bending) modes of the upper state. The widths of the peaks in the spectrum are influenced by the shape of the saddle point along the asymmetric stretch coordinate of the upper surface, which governs the lifetime of the upper state with respect to dissociation.

The identification of the dissociating O_3^- state is uncertain. Theoretical calculations[4,5] have predicted two low-lying excited states, $1\ ^2A_1$ and $1\ ^2A_2$, to which dipole-allowed transitions are possible from the ground $X\ ^2B_1$ state. The $1\ ^2A_1 \leftarrow X\ ^2B_1$ transition occurs at the lower photon energy, but previous investigations[12,15] have attributed the visible absorption band to $1\ ^2A_2 \leftarrow X\ ^2B_1$. The basis for this assignment has been that the $1\ ^2A_2 \leftarrow X\ ^2B_1$ transition has been observed[36] in ClO_2 with a threshold at 2.606 eV. Such an analogy has limitations, however, since the spectrum of the $1\ ^2A_2 \leftarrow X\ ^2B_1$ transition in ClO_2 is not diffuse,[38] even though the entire spectrum appears at photon energies above the dissociation energy of the ground state (2.50 eV).

An unambiguous assignment of the dissociating state could be obtained from a measurement of the angular distribution of O^- photofragments. For the case of $^2A_1 \leftarrow {}^2B_1$, the O^- distribution would be isotropic in the plane perpendicular to the direction of laser polarization, whereas the distribution of fragments from $^2A_2 \leftarrow {}^2B_1$ would have more parallel character. An angular distribution measurement would also provide a check on the direct dissociation model by probing the lifetime of the dissociating state.[39] In contrast to the case[40] of CO_3^-, such a distribution cannot be obtained for O_3^- in the drift tube apparatus. The numerous collisions, caused by the much higher neutral gas densities required for O_3^- formation, would randomize the initial angular distribution of O^- photofragments prior to their detection. Consequently, this question must be investigated in the future using a beam[41] apparatus.

VI. Bond Energy

Since photodissociation is observed from the lowest level of the O_3^- excited state, the thresholds of 2.146 or 2.163 eV reported here provide only an upper limit to the dissociation energy $D_o(O_2\text{-}O^-)$ of the $O_3^-(X^2B_1)$ state. The actual dissociation energy could, in principle, be obtained from a measurement of the kinetic energy of the O^- photofragments and a knowledge of the internal energy of the corresponding O_2 product. In the absence of these more direct data, $D_o(O_2\text{-}O^-)$ can be related to the dissociation energy of O_3 and the electron affinities of O and O_3 by the equation:

$$D_o(O_2\text{-}O^-) = EA(O_3) + D_o(O_2\text{-}O) - EA(O) \quad . \qquad (4)$$

The threshold for O_3^- photodetachment has been measured[24] to be 1.99 ± 0.1 eV. This value represents an upper limit to $EA(O_3)$, since the Franck-Condon factors for the $O_3(X^1A_1) \leftarrow O_3^-(X^2B_1)$ transition are not sufficiently well known to ensure that the product neutral is not produced with internal energy at the photodetachment threshold. The electron affinity has also been deduced from the kinetic energy thresholds for O_3^- formation in reactions of various species with O_3. The reactants used in these studies were (I^-),[21] ≥ 1.96 eV; (Cs),[22] 2.14 ± 0.15 eV; (F^-, Br^-, Cl^-, I^-, CO_3^-),[23] 2.15 ± 0.15 eV; and (OH^-),[19] ≥ 1.8234 eV. Provided the O_3 molecule does not have significant internal energy at the time of reaction, these measurements represent lower limits to $EA(O_3)$, since the product O_3^- ion may be formed with internal energy. Combining the photodetachment and reaction values, the electron affinity of O_3 is determined to be

2.06 $\pm$ 0.06 eV. This value is also consistent with those obtained by a theoretical calculation[2] and crystallographic studies.[42]

Using the above value for $EA(O_3)$ and the recommended values for $EA(O)$[43] and $D(O_2\text{-}O)$[44] of $1.462\ ^{+0.003}_{-0.007}$ eV and 1.05 $\pm$ 0.02 eV, respectively, the dissociation energy of the $O_3^-(X^2B_1)$ state is found from Eqn. (4) to be 1.65 $\pm$ 0.06 eV.

It has been pointed out[19] that if the above values are all correct within their stated uncertainties, a significant discrepancy exists regarding either the dissociation energy of CO_3^-, $D(CO_2\text{-}O^-)$, or of O_3^-. From reaction rate studies, the difference in the dissociation energies of CO_3^- and O_3^- was determined[19] to be <u>at least</u> 0.58 eV, while the photodissociation of CO_3^- led[40] to an <u>upper limit</u> of 1.9 eV for the dissociation energy of CO_3^-. These two values place an <u>upper limit</u> on the dissociation energy of O_3^- of 1.32 eV, in clear disagreement with the value of 1.65 eV obtained above. It is not yet known if one of the numbers quoted above is significantly in error, or if several of them are slightly in error in such a way as to account for the 0.3 eV discrepancy.

VII. Summary

The O_3^- photodestruction cross section has been measured over a wavelength range of 6400-5080 Å. The ion photodissociates in this region to form $O^- + O_2$ with a cross section that exhibits structure consistent with dissociation from vibrational levels of an excited electronic state. Progressions in the symmetric stretch and bending modes of the excited state

are identified and transitions originating from these modes in the X^2B_1 state are observed. It is found that the structure in the cross section can be explained by either of two sets of vibrational frequencies for these states. The assignments, given in Table 1, fix the origin of the excited state at either 2.146 or 2.163 eV above the X^2B_1 state. The identity of the dissociating state is not experimentally established; however, recent calculations indicate that it is either the 1^2A_1 or 1^2A_2.

Evidence is found for the formation of vibrationally excited O_3^- in the reaction $O^- + 2O_2 \rightarrow O_3^- + O_2$. Relaxation of the excited ion in O_2 is observed with an apparent rate coefficient of 10^{-14} cm^3 s^{-1}.

TABLE I: Summary of O_3^- Molecular Constants

Source	Ground State X^2B_1			Excited State ($^2A_1$, $^2A_2$)			
	ω''_1	ω''_2	ω''_3	ω'_1	ω'_2	ω'_3	T_o (eV)
This work (I)	790	419		855	290		2.146
(II)	928	403		794	282		2.163
matrix[a]				834-908	~ 300		2.183-2.254
matrix[b]			802.0	818			
matrix[c]	1012-1026						
matrix[d]		553.6-618.6	786.7-814.3				
crystal[e]	1016-1029			857			
Liquid Ammonia[f]				~ 820	~ 400		~ 2.19
ClO_2[g]	963.5	451.7	1133.0	722.4	296.3	780.1	2.449

a. Ref. 15
b. Ref. 11, 12
c. Ref. 14
d. Ref. 13
e. Ref. 7,8
f. Ref. 10
g. Ref. 36

REFERENCES

*This research was supported by the U. S. Army Ballistic Research Laboratory through the U. S. Army Research Office, and by the U. S. Air Force Office of Scientific Research.

1. L. Thomas, Radio Sci. 9, 121 (1974); F. E. Niles and M. G. Heaps, Third General Scientific Assembly of the International Association of Geomagnetism and Aeronomy: Abstracts of Papers (Seattle, 1977), p. 58.
2. M. M. Heaton, A Pipano, and J. J. Kaufman, Int. J. Quantum Chem. 6, 181 (1972).
3. J. M. Sichel, Can. J. Chem. 51, 2124 (1973).
4. D. G. Hopper, W. B. England, P. J. Fortune, B. J. Rosenberg, P. Benioff, G. Das, and A. C. Wahl, 30th Symposium on Molecular Structure and Spectroscopy: Abstracts of Papers (Ohio State U., Columbus, Ohio, 1975), p. 84; A. C. Wahl, W. B. England, B. J. Rosenberg, D. G. Hopper, and P. J. Fortune, "Theoretical Studies of the Atmospheric Triatomic Molecules H_2O, N_2O, NO_2, CO_2, O_3 and Their Ions," Argonne National Lab. Rep. ANL-77-3 (Argonne National Lab, Argonne, Ill., 1977).
5. T. H. Dunning and P. J. Hay, 31st Symposium on Molecular Structure and Spectroscopy: Abstracts of Papers (Ohio State U., Columbus, Ohio, 1976), p. 118; T. H. Dunning, private communication, 1975.
6. A. D. McLachlan, M. C. R. Symons, and M. G. Townsend, J. Chem. Soc. (Lond.) 1959, 952 (1959).
7. J. B. Bates, Chem. Phys. Letters 26, 75 (1974).

8. J. B. Bates and J. C. Pigg, J. Chem. Phys. 62, 4227 (1975).

9. I. J. Solomon, A. J. Kacmarek, J. M. McDonough, and K. Hattori, J. Am. Chem. Soc. 82, 5640 (1960).

10. P. A. Giguere and K. Herman, Can. J. Chem. 52, 3941 (1974).

11. M. E. Jacox and D. E. Milligan, Chem. Phys. Letters 14, 518 (1972).

12. M. E. Jacox and D. E. Milligan, J. Mol. Spectry. 43, 148 (1972).

13. R. C. Spiker and L. Andrews, J. Chem. Phys. 59, 1851 (1973).

14. L. Andrews and R. C. Spiker, J. Chem. Phys. 59, 1863 (1973).

15. L. Andrews, J. Chem. Phys. 63, 4465 (1975).

16. L. G. McKnight, Phys. Rev. A 2, 762 (1970).

17. R. M. Snuggs, D. J. Volz, I. R. Gatland, J. H. Schummers, D. W. Martin, and E. W. McDaniel, Phys. Rev. A 3, 487 (1971).

18. F. C. Fehsenfeld and E. E. Ferguson, J. Chem. Phys. 61, 3181 (1974).

19. I. Dotan, J. A. Davidson, G. E. Streit, D. L. Albritton, and F. C. Fehsenfeld, J. Chem. Phys. 67, xxxx (1977).

20. R. K. Curran, J. Chem. Phys. 35, 1849 (1961).

21. J. Berkowitz, W. A. Chupka, and D. Gutman, J. Chem. Phys. 55, 2733 (1971).

22. E. W. Rothe, S.Y. Tang, and G. P. Reck, J. Chem. Phys. 62, 3829 (1975).

23. C. Lifshitz, R. L. C. Wu, and T. O. Tiernan, J. Chem. Phys. (submitted for publication).

24. S. F. Wong, T. V. Vorburger, and S. B. Woo, Phys. Rev. A 5, 2598 (1972).

25. P. C. Cosby, R. A. Bennett, J. R. Peterson, and J. T. Moseley, J. Chem. Phys. 63, 1612 (1975).

26. P. C. Cosby, J. H. Ling, J. R. Peterson, and J. T. Moseley, J. Chem. Phys. 65, 5267 (1976).

27. J. T. Moseley, P. C. Cosby, R. A. Bennett, and J. R. Peterson, J. Chem. Phys. 62, 4826 (1975).

28. L. M. Chanin, A. V. Phelps, and M. A. Biondi, Phys. Rev. 128, 219 (1962).

29. L. M. Branscomb, S. J. Smith, and G. Tisone, J. Chem. Phys. 43, 2906 (1965).

30. R. M. Snuggs, D. J. Volz, J. H. Schummers, D. W. Martin, and E. W. McDaniel, Phys. Rev. A 3, 477 (1971).

31. J. A. Vanderhoff, J. Chem. Phys. 67, xxxx (1977).

32. B. A. Huber, P. C. Cosby, J. R. Peterson, and J. T. Moseley, J. Chem. Phys. 66, 4520 (1977).

33. C. W. von Rosenberg and D. W. Trainor, J. Chem. Phys. 61, 2442 (1974); ibid. 63, 5348 (1975).

34. D. I. Rosen and T. A. Cool, J. Chem. Phys. 62, 466 (1975).

35. K. K. Hui, D. I. Rosen, and T. A. Cool, Chem. Phys. Letters 32, 141 (1975).

36. G. Herzberg, Molecular Spectra and Molecular Structure III. Electronic Spectra and Electronic Structure of Polyatomic Molecules (Van Nostrand Reinhold Co., New York, 1966).

37. R. T. Pack, J. Chem. Phys. 65, 4765 (1976).

38. J. B. Coon, J. Chem. Phys. 14, 665 (1946).

39. R. N. Zare and D. R. Herschbach, Proc. IEEE 51, 173 (1963).

40. J. T. Moseley, P. C. Cosby, and J. R. Peterson, J. Chem. Phys. 65, 2512 (1976).

41. B. A. Huber, T. M. Miller, P. C. Cosby, H. D. Zeman, R. L. Leon, J. T. Moseley, and J. R. Peterson, Rev. Sci. Instr. (in press).

42. R. H. Wood and L. A. D'Orazio, J. Chem. Phys. 69, 2562 (1965).

43. H. Hotop and W. C. Lineberger, J. Phys. Chem. Ref. Data 4, 539 (1975).

44. J. L. Gole and R. N. Zare, J. Chem. Phys. 57, 5331 (1972).

FIGURE CAPTIONS

1. Total photodestruction cross section of O_3^- as a function of photon energy. The predominant process observed is photodissociation into $O^- + O_2$. The ordinate has been expanded by a factor of five for the data in the wavelength range of 6200-5700 Å.

2. Drift distance dependence of the O_3^- photodestruction cross section at five wavelengths.

3. Total photodestruction cross section of O_3^- as a function of photon energy. The upper and lower sets of data were obtained at drift distances of 10.2 and 30.5 cm, respectively. For clarity, the upper data have been displaced along the ordinate by a factor of two. Transitions $(10 \leftarrow 0\, v_2')$ and $(11 \leftarrow 0 v_2')$ arising from excited stretching modes of the X^2B_1 state which are expected from assignments I and II are given by the lines in the upper and lower halves of the figure.

4. Photodestruction cross section of O_3^- as a function of photon energy showing the assignment of transitions to two vibrational modes of the dissociating electronic state. Transitions arise from both the ground vibrational levels $(00 \leftarrow v_1'\ v_2')$ and from the first excited bending mode $(01 \leftarrow v_1'\ v_2')$ of the X^2B_1 state. Assignments made from frequency set I are shown in the upper part of the figure while those from set II are in the lower part.

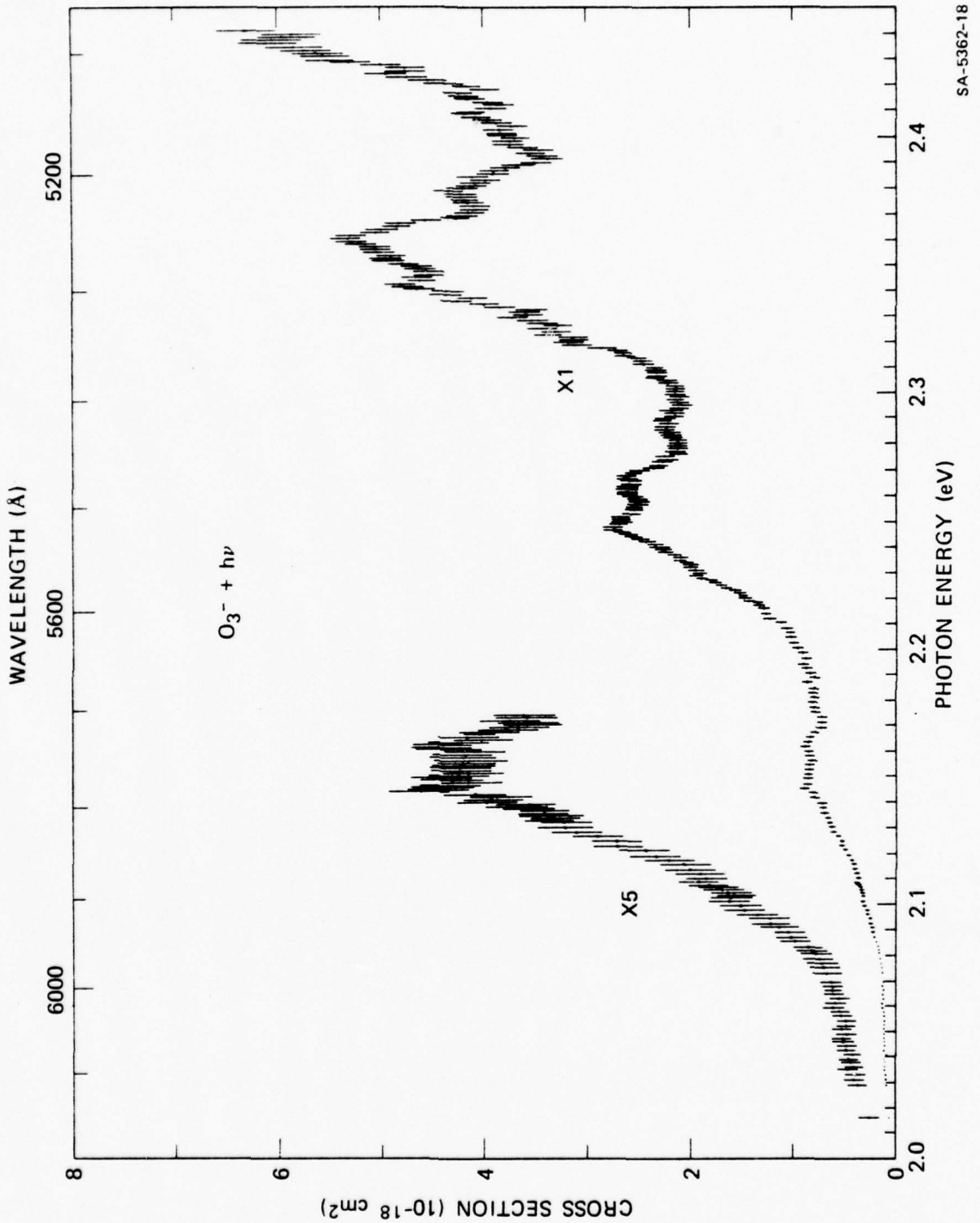

Fig. 1
Cosby, Moseley,
Peterson, & Ling

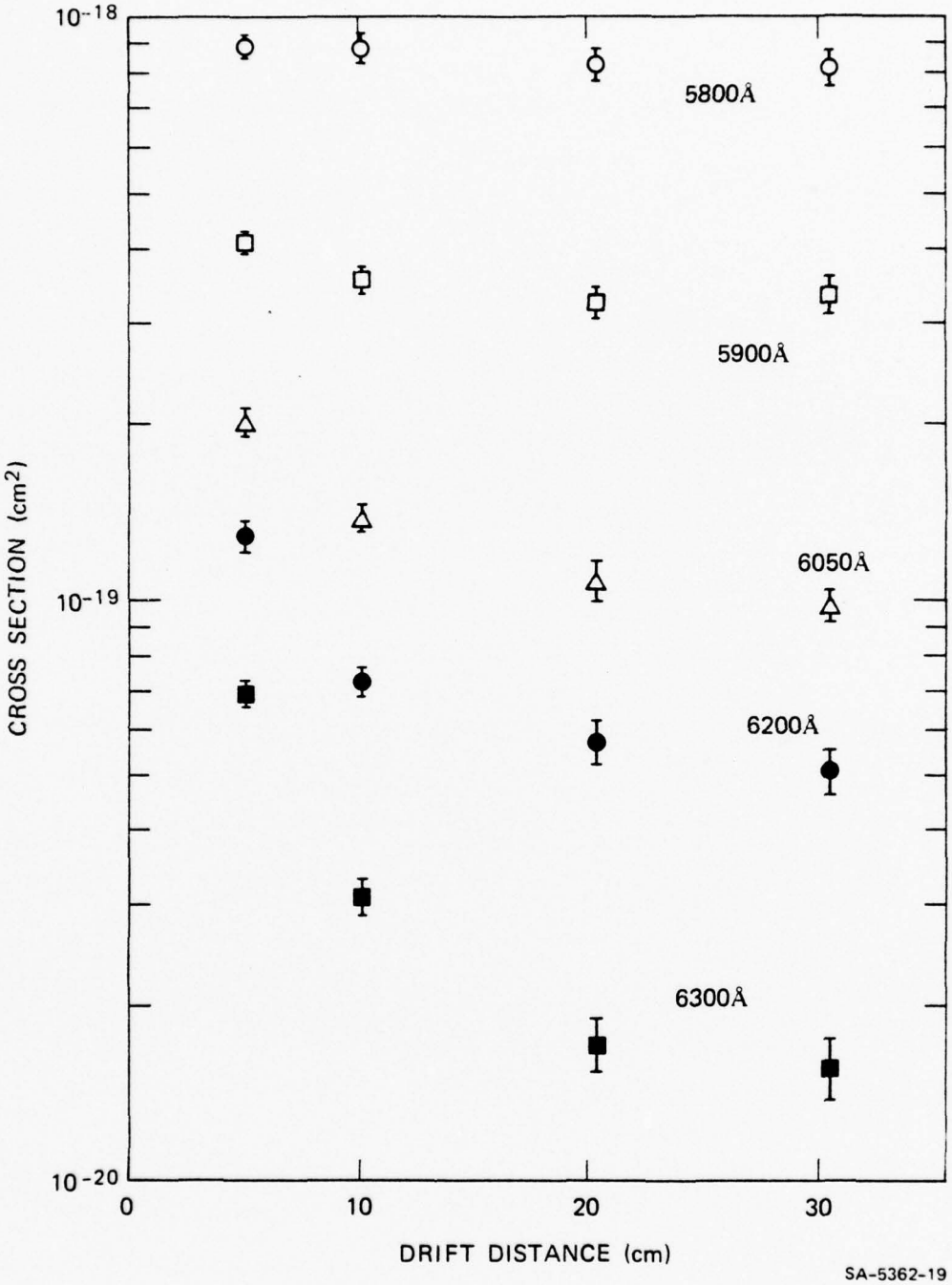

Fig. 2
Cosby, Moseley,
Peterson, & Ling

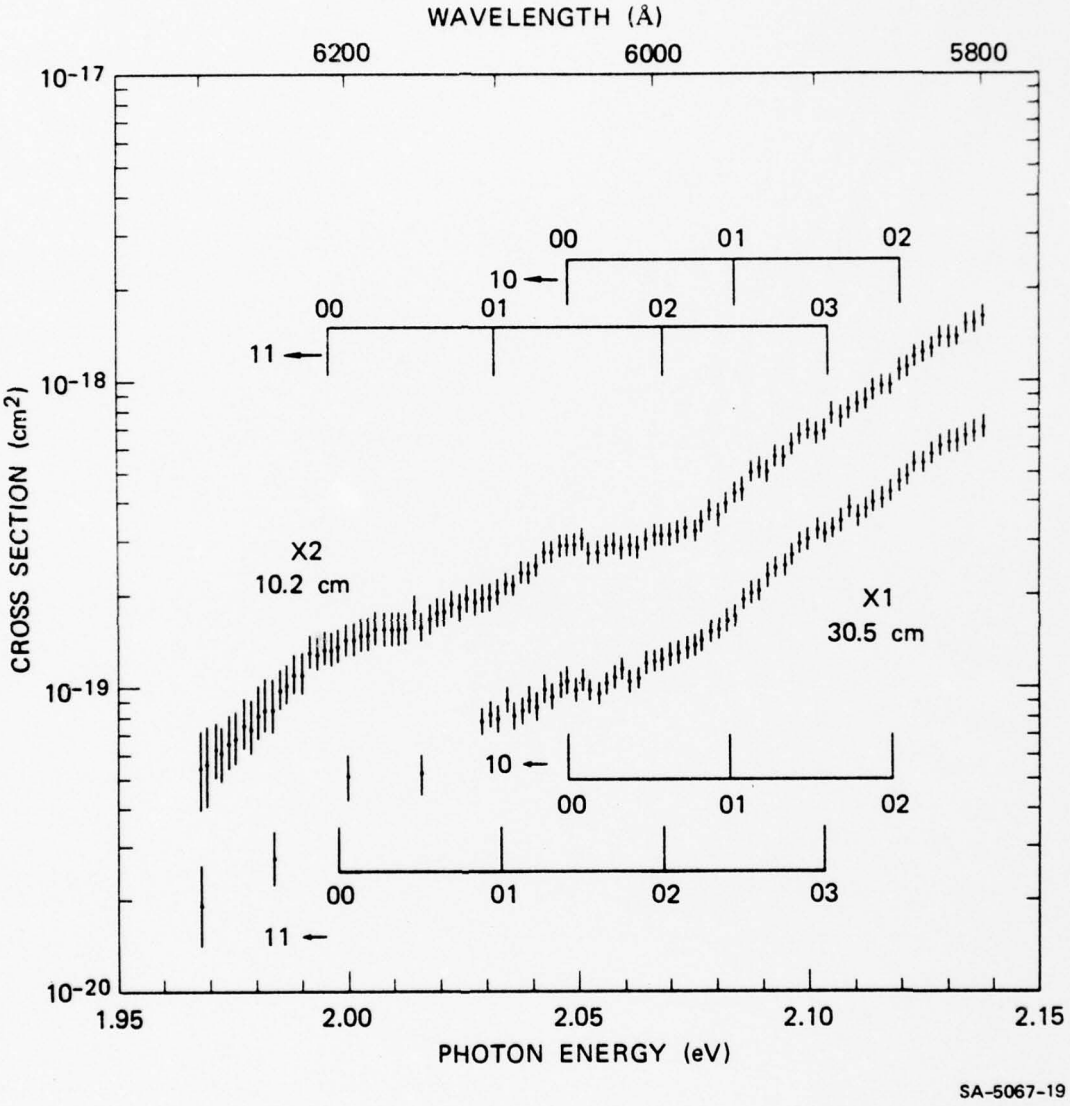

Fig. 3
Cosby, Moseley,
Peterson, & Ling

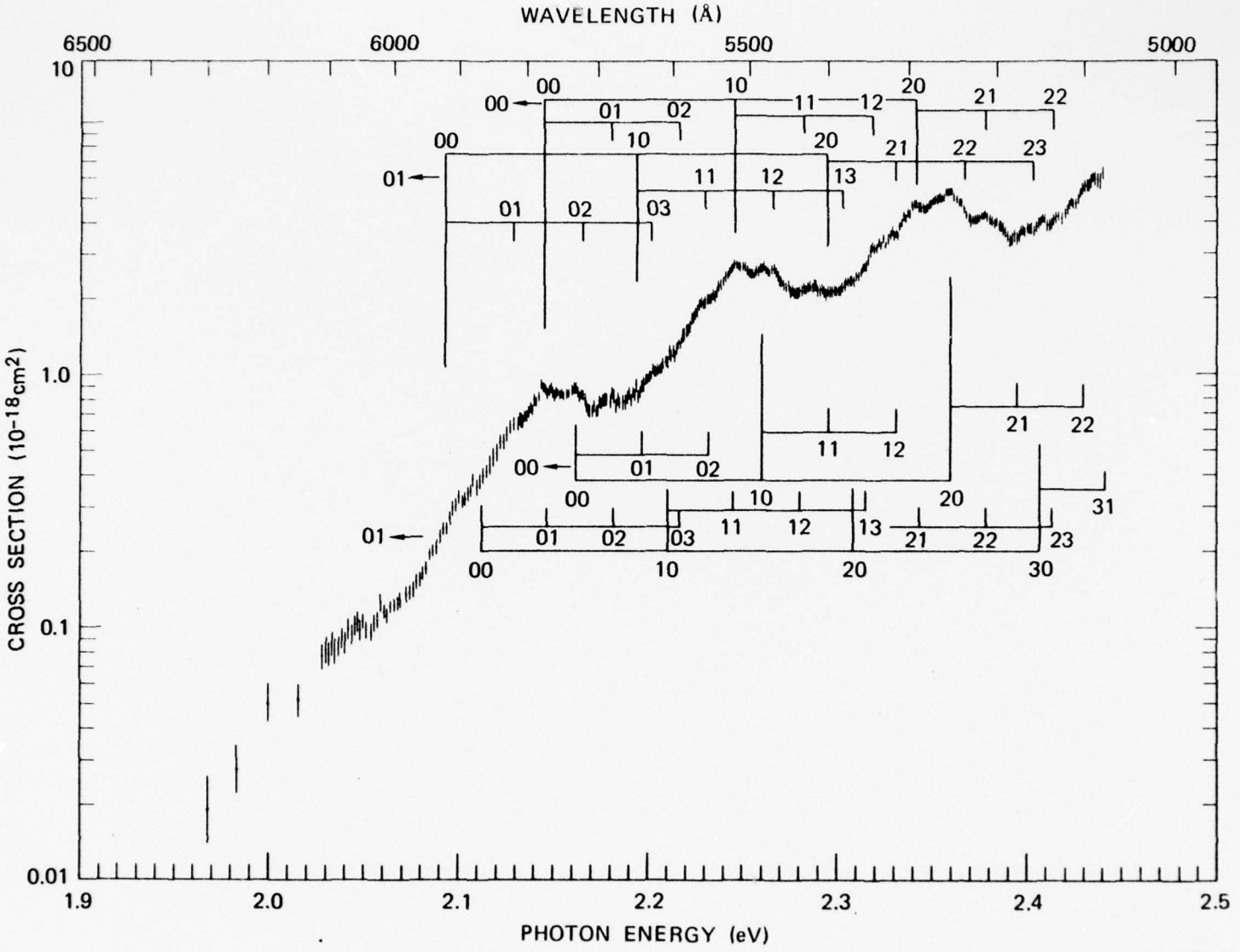

Fig. 4
Cosby, Moseley,
Peterson, & Ling

APPENDIX E

PHOTODISSOCIATION AND PHOTODETACHMENT OF MOLECULAR NEGATIVE IONS. IV. HYDRATES OF O_3^-

P. C. Cosby, G. P. Smith, and J. T. Moseley
Molecular Physics Center
SRI International, Menlo Park, CA 94025

ABSTRACT

The total photodestruction cross sections of gas-phase $O_3^- \cdot H_2O$ and $O_3^- \cdot 2H_2O$ have been measured over a wavelength range of 6300-5120 Å using a tunable dye laser. The cross sections for these ions closely resemble that of O_3^-, but are progressively smaller, blue-shifted, and less structured with the addition of each water ligand. The major product of the $O_3^- \cdot H_2O$ photodestruction is O_3^-. The possibility of other dissociation channels in the hydrate photodestruction and the influence of the water ligands on the O_3^- absorption spectrum are discussed.

MP 77-113

INTRODUCTION

Molecular ion hydrates are generally considered to be weakly bound complexes held together primarily by the electrostatic attraction between the ion and the permanent dipole moment of the water molecule. Such species are abundant in the lower regions of the ionosphere.[1] Most of the present knowledge of the hydrates has been obtained from gas-phase ion-molecule reaction rate measurements. Studies of the equilibrium reactions of the parent ions with H_2O have yielded energies for the ion-water bond of approximately 0.5 eV.[2,3] In a few instances the addition of a single water molecule to a molecular ion has dramatically altered the ion-molecule reactions of the hydrate from those observed for the isolated ion.[3] Detailed theoretical calculations have thus far been limited to the interaction of atomic ions with the water molecule.[4] No information exists concerning the effect of the water molecule on the electronic states of a molecular ion in the gas phase.

RESULTS

We report here the measurement of the total photodestruction cross sections of the ions $O_3^- \cdot H_2O$ and $O_3^- \cdot 2H_2O$ using a drift tube mass spectrometer coupled with a tunable dye laser.[5] The ions were produced in O_2 gas containing a trace ($\sim$ 200 ppm) of water vapor by the three-body reactions[3]

$$O_3^- + H_2O + O_2 \rightarrow O_3^- \cdot H_2O + O_2 \qquad (1)$$

and

$$O_3^- \cdot H_2O + H_2O + O_2 \rightleftarrows O_3^- \cdot 2H_2O + O_2 \quad . \tag{2}$$

At an O_2 pressure of 0.5 torr, a drift distance of 20.3 cm, and an E/N of 5×10^{-17} V-cm^2, the ratio of the ions O_3^-, $O_3^- \cdot H_2O$, and $O_3^- \cdot 2H_2O$ in the drift tube was approximately 100:10:1.

The total photodestruction cross sections[6] of O_3^-, $O_3^- \cdot H_2O$, and $O_3^- \cdot 2H_2O$ are shown in Fig. 1 for the wavelength region of 6300-5120 Å. For clarity, the data for the first and second hydrates have been displaced along the ordinate from those of O_3^- by factors of 10 and 100, respectively. The cross sections for O_3^- are taken from the preceeding paper.[6] The error bars for each of the data points in this figure represent one standard deviation of statistical error. The uncertainty in the absolute value of each of the cross sections is ± 12%.

The previously stated drift tube conditions were chosen to minimize coupling[7] of the photon reactions of any one of these species to the others via Reactions (1) and (2). These conditions, however, also permit formation of the hydrates along the entire drift distance. Thus, it is not possible to insure the hydrates were in a thermal ($\sim 300^\circ$K) distribution of internal energy states at the time of photon interaction.

DISCUSSION

We observe the production of photofragment O_3^- ions from the photodestruction of $O_3^- \cdot H_2O$. Since the concentration of the hydrate was always an order of magnitude smaller than the concentration of O_3^- produced in the drift tube, it is not possible to state with certainty that the reaction

$$O_3^- \cdot H_2O + h\nu \rightarrow O_3^- + H_2O \tag{3}$$

is the only channel for the photodestruction at these wavelengths. However, since the neutral $O_3 \cdot H_2O$ would not be expected to be bound by other than van der Waals forces, photodetachment of the $O_3^- \cdot H_2O$ can be ruled out; the threshold for this process could occur only at photon energies equal to or greater than the sum of the electron affinity of O_3 (2.06 eV)[6] plus the dissociation energy of the $O_3^- - H_2O$ bond ($\sim$ 0.5 eV).[3] The photodissociation channel

$$O_3^- \cdot H_2O + h\nu \rightarrow O^- + O_2 + H_2O \qquad (4)$$

cannot, however, be eliminated since the dissociation energy of the $O^- - O_2$ bond is expected[6] to be only 1.65 $\pm$ 0.06 eV. Thus, the energetic threshold for such a process would be fully consistent with that observed in Fig. 1.

The products of the $O_3^- \cdot 2H_2O$ photodestruction reaction were not experimentally observed, since this ion is formed only in trace concentrations in the drift tube. The photodissociation processes

$$O_3^- \cdot 2H_2O + h\nu \begin{array}{l} \rightarrow O_3^- \cdot H_2O + H_2O \\ \rightarrow O_3^- + H_2O + H_2O \end{array} \rightarrow O^- \cdot H_2O + O_2 + H_2O \qquad (5)$$

are all probably energetically accessible, but the threshold for either photodetachment or photodissociation into $O^- + 2H_2O + O_2$ should occur at higher photon energies than were used here.

As seen in Fig. 1, the cross sections for the hydrates strongly resemble that of O_3^-. Note, however, that the spectra of the hydrates show progressively less structure with the addition of each water ligand and are shifted by 0.60 $\pm$ 0.005 eV and 0.072 $\pm$ 0.005 eV to higher photon energy than

that of O_3^-. Also, the addition of each water of hydration results in a reduction in the cross section magnitude by approximately 25%.

The O_3^- photodissociation spectrum has been interpreted[6] as resulting from absorptions from the ground electronic state of the ion into two vibrational modes of an excited electronic state which dissociates. The close similarities in the photodestruction spectra of O_3^- and its hydrates indicates that the bonding of the water molecule only slightly perturbes the O_3^- energy levels from those of the isolated ion. The small shifts of the structure in the hydrate cross sections to higher photon energies reflect the relative interaction of the water molecule with the ground and excited O_3^- electronic states. The increasing diffuseness of the features in the hydrate cross section likely results from the increasing number of vibrational modes present in the hydrates. Since the energy level spacing of many of these additional modes will be small and a number of the levels in each mode will be populated in the hydration reaction, a broadening of the spectral features in the absorption should be expected. Similarly, the small decreases in the cross section magnitude with the addition of each water to the O_3^- could reflect small changes in the transition moment for the absorption. Nevertheless, reactions (3) and (5) each require intramolecular transfer of the energy deposited in the $O^- - O_2$ bond by absorption of a photon into the ion-water bond which is broken during dissociation of the hydrate. One can thus not rule out competition between photodissociation and fluorescence, which is not expected for the direct dissociation observed[6] in the isolated O_3^- ion, as the cause of the smaller cross sections in the hydrates.

REFERENCES

*Research supported by the U.S. Army Ballistic Research Laboratory through the Army Research Office.

1. J. N. Rowe, A. P. Mitra, A. J. Ferraro, and H. S. Lee, J. Atmos. Terr. Phys. 36, 755 (1974).

2. M. Arshadi, R. Yamdagni, and P. Kebarle, J. Phys. Chem. 74, 1475 (1970); J. D. Payzant, P. Yamdagni, and P. Kebarle, Can. J. Chem. 49, 3309 (1971); M. French, L. P. Hills, and P. Kebarle, Can. J. Chem. 51, 456 (1973).

3. F. C. Fehsenfeld and E. E. Ferguson, J. Chem. Phys. 61, 3181 (1974).

4. K. G. Spears, J. Chem. Phys. 57, 1850 (1972); H. Kistenmacher, E. Popkie, and E. Clementi, J. Chem. Phys. 59, 5842 (1973).

5. P. C. Cosby, J. H. Ling, J. R. Peterson, and J. T. Moseley, J. Chem. Phys. 65, 5267 (1976).

6. P. C. Cosby, J. T. Moseley, J. R. Peterson, and J. H. Ling, J. Chem. Phys. (preceeding paper).

7. G. P. Smith, P. C. Cosby, and J. T. Moseley, J. Chem. Phys. 67, xxxx (1977) (15 Oct 77).

FIGURE CAPTIONS

1. Total photodestruction cross sections for O_3^-, $O_3^- \cdot H_2O$, and $O_3^- \cdot 2H_2O$ as a function of photon energy. For clarity, the data for the single and double hydrates have been lowered by factors of 10 and 100, respectively, relative to the cross section scale of O_3^-.

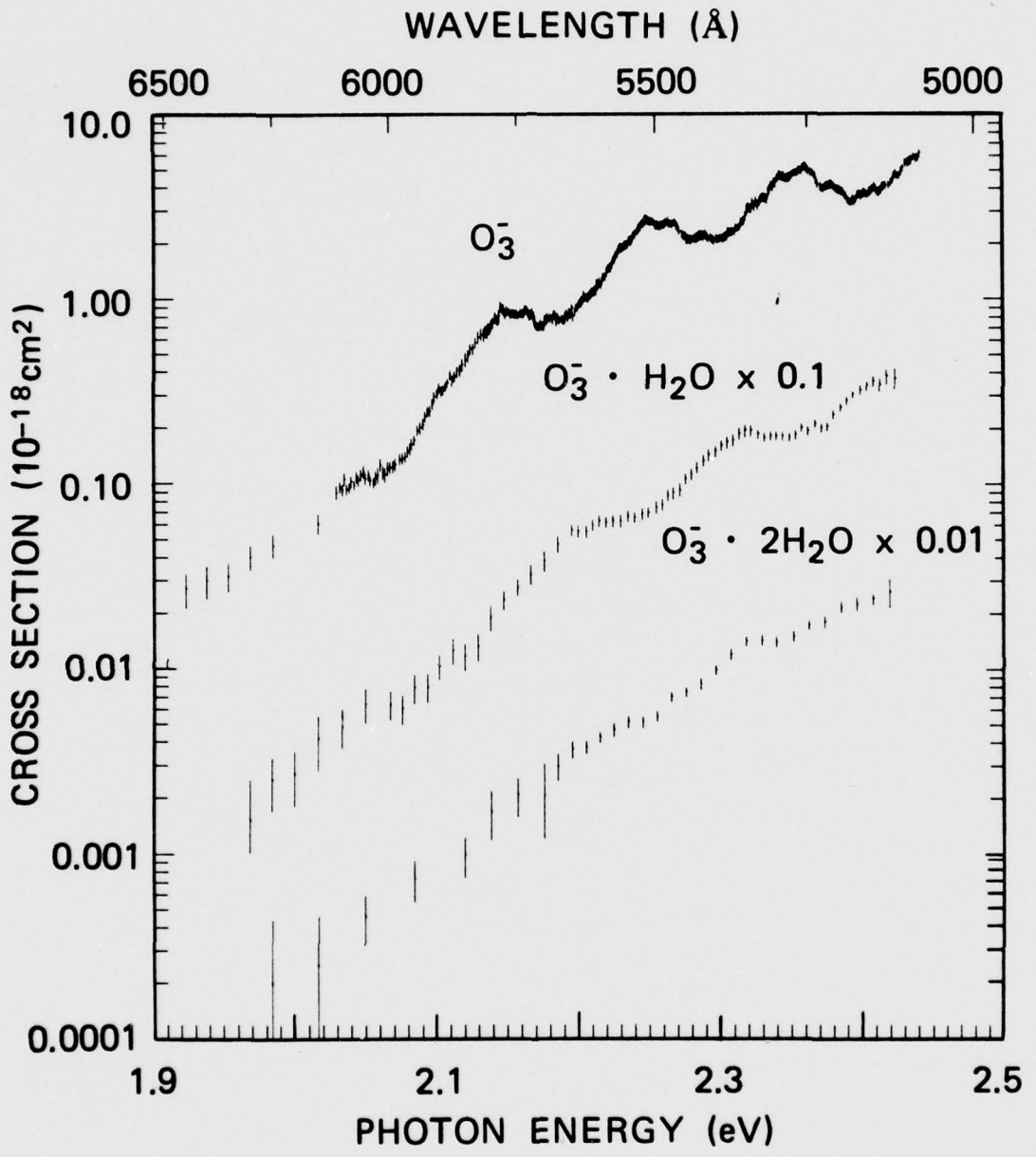
WAVELENGTH (Å)
6500
6000
5500
5000
10.0
1.00
0.10
0.01
0.001
0.0001
CROSS SECTION (10^{-18}cm^2)
O_3^-
$O_3^- \cdot H_2O \times 0.1$
$O_3^- \cdot 2H_2O \times 0.01$
1.9
2.1
2.3
2.5
PHOTON ENERGY (eV)
SA-5067-18

Figure 1

APPENDIX F

PHOTODISSOCIATION AND PHOTODETACHMENT OF MOLECULAR NEGATIVE IONS V. ATMOSPHERIC IONS FROM 7000 TO 8400 Å*

G. P. Smith, L. C. Lee, P. C. Cosby, J. R. Peterson, and J. T. Moseley

Molecular Physics Center, SRI International
Menlo Park, California 94025

ABSTRACT

Measurements of the photodestruction cross sections for a number of parent and first hydrate negative ions of atmospheric importance have been extended to the wavelength range from 7000 to 8400 Å, using a drift tube mass spectrometer and a tunable dye laser. Most of these ions do not dissociate or detach at these wavelengths; upper limits smaller than 1.0×10^{-19} *cm*^{2} are established for the photodestruction cross sections of O_3^-, $O_2^- \cdot H_2O$, $O_3^- \cdot H_2O$, CO_3^-, CO_4^-, $CO_4^- \cdot H_2O$, HCO_3^-, $HCO_3^- \cdot H_2O$, $O_2^- \cdot NO$, $O_2^- \cdot NO \cdot H_2O$, and $NO_2^- \cdot H_2O$. Thresholds for the photodestruction of $CO_3^- \cdot H_2O$ and O_4^- are observed at photon energies of 1.67 eV and 1.57 eV respectively, and the cross sections for these ions have been measured at higher photon energies.

*This research was supported by the U.S. Army Ballistics Research Laboratories through the U.S. Army Research Office.

MP 77-115

I INTRODUCTION

In recent years, the importance of molecular negative ions in D-region ionospheric chemistry has been noted.[1] Photodestruction of ions which can be formed in various mixtures of atmospheric gases affects the D-region electron density and ion composition. Such processes are also important in gas discharge lasers,[2] as well as being of fundamental interest in the study of the electronic structure of negative ions. In previous work[3-5] we have studied photodestruction processes of atmospheric ions at wavelengths between 5100 and 7000 Å. The present work extends this wavelength range to the near infrared (8400 Å), and suggests very small or zero negative ion photodestruction cross sections farther in the infrared.

Specifically, this paper will present upper limits for the photodestruction cross sections of the following atmospheric negative ions between 7000 and 8400 Å: O_3^-, $O_2^- \cdot H_2O$, $O_3^- \cdot H_2O$, CO_3^-, CO_4^-, $CO_4^- \cdot H_2O$, HCO_3^-, $HCO_3^- \cdot H_2O$, NO_3^-, $O_2^- \cdot NO$, $O_2^- \cdot NO \cdot H_2O$, and $NO_2^- \cdot H_2O$. Measurements were made to threshold for O_4^- and $CO_3^- \cdot H_2O$. Recent measurements between 5100 and 7000 Å of photodissociation processes for nitrogen-containing atmospheric negative ions,[6] and for the hydrates of O_3^- [7], and measurements[8] of the photodetachment of OH^-, O^-, and O_2^- relative to D^- between 5100 and 8600 Å will be reported separately.

II APPARATUS AND TECHNIQUE

The experimental measurements were made on a drift tube mass spectrometer coupled with a tunable dye laser apparatus which has been described.[3,4] Negative ions, formed by electron attachment in the source region and by subsequent ion-molecule reactions, drift down the tube under the influence of a weak electric field. Since the drift distance was typically 20.3 cm, the ions undergo many thermalizing collisions after formation. Pressures between 0.10 and 0.50 torr were utilized, and the applied field was sufficiently weak that the drift velocity was only about one-tenth thermal velocity (E/N = 10 Td). Approximately 1 mm before the exit aperture in the end plate of the drift tube, the ions traverse the cavity of a chopped, tunable dye laser. Ions which pass through the aperture into a high vacuum region are mass selected, detected, and accumulated by a two-channel counter (laser on and laser off) until the desired statistical accuracy is obtained.

For the current red wavelength work, the dye laser is pumped by 3.5 W of the 6471 and 6764 Å lines of a krypton ion laser. The dyes[9] oxazine and DEOTC were used for the wavelengths 7000-7800 Å and 7800-8600 Å, respectively. Intracavity power levels of 7 to 30 W were obtained using oxazine, while DEOTC provided up to 5 W. Due to the difficulty of working in the infrared and the lack of observable photodestruction, attempts to extend measurements to longer wavelengths with other dyes were not made. A few measurements were also made at 6800 Å using rhodamine 640[9], pumped by the yellow and green lines of the krypton laser.

Accurate measurements require that attention be paid to the conditions of ion production along the drift tube. Past work has demonstrated that measured photodestruction cross sections can be affected by equilibrium reactions with other photoabsorbing species[10] and by vibrational excitation.[3,11] Equilibrium problems are negligible here since no photodissociating or photodetaching species were present under most operating conditions. Previously investigated[3-5] drift tube conditions were used for the production of the ions of interest and are listed in Table I. For all measurements of hydrated ions, the partial pressure of water was kept below that which would produce significant quantities of the second hydrate.

All cross sections reported here are determined by normalization[3] to the O^- photodetachment cross sections of Branscomb et al.,[12] using the equation

$$\sigma_{A^-}(\lambda) = \sigma_{O^-}(\lambda) \frac{\ln(I_o/I)_{A^-} \; P_{O^-} \; v_{A^-}}{\ln(I_o/I)_{O^-} \; P_{A^-} \; v_{O^-}} \qquad (1)$$

where P is the measured laser output power and v is the drift velocity calculated from the reduced mobility.[13]

III $CO_3^- \cdot H_2O$ PHOTODISSOCIATION

A large photodissociation cross section for $CO_3^- \cdot H_2O$ has been reported[5] at wavelengths shorter than 7000 Å. We have extended these measurements to 7600 Å and observed a threshold at 1.67 ± .03 eV (7400 Å). This is the highest photon energy for which a cross section less than

1×10^{-19} cm^2 (one standard deviation) and consistent with zero was measured. Figure 1 shows the results of these new measurements, and those of Ref. 3 for the processes:

$$CO_3^- \cdot H_2O + h\nu \rightarrow CO_3^- + H_2O \quad \Delta H = 0.5 \text{ eV}^{14} \tag{2}$$

$$\text{and } CO_3^- + h\nu \rightarrow O^- + CO_2 \quad \Delta H = -1.8 \text{ eV}^{15} \tag{3}$$

The sharp decline in the $CO_3^- \cdot H_2O$ cross section above 7000 Å is quite apparent. The nature of the photodestruction processes, the electronic transition, and the fact that the hydrate cross section is larger and less structured have been discussed previously.[5]

These new results yield direct information on the threshold for $CO_3^- \cdot H_2O$ photodissociation, and more indirectly, information on the excited states and bonding of CO_3^- and its first hydrate. The data can best be discussed in comparison to our recent work[7] on O_3^- and its first two hydrates. There we observed nearly identical photodissociation cross sections for O_3^- and its hydrates, except that the cross section for the first hydrate was shifted to 0.06 eV higher photon energy, and that for $O_3^- \cdot 2H_2O$ to approximately 0.09 eV higher energy. The structure observed in the O_3^- cross sections became progressively more diffuse with the addition of each water of hydration. A major difference between the photodissociation of CO_3^- and that of O_3^- is that for O_3^- essentially all of the absorption in this wavelength range results in photodissociation,[7] while for CO_3^- apparently only a part of the absorption results in dissociation[15] above the thermodynamic limit of 1.8 eV.

The CO_3^- absorption almost certainly continues down to the excited state origin of 1.52 eV, with no photodissociation.

The fact that the cross sections for O_3^- and its hydrates are nearly identical shows[7] that the weak $O_3^- \cdot H_2O$ bond only slightly perturbs the O_3^- electronic states. It is very likely that the CO_3^- electronic states are also only slightly perturbed by hydration. The difference in the magnitudes of the CO_3^- and $CO_3^- \cdot H_2O$ cross sections apparently occurs because a larger fraction of the total absorption results in dissociation for the hydrates, due to the availability of a much lower energy product channel, $CO_3^- + H_2O$. This can also explain why the hydrate cross section continues to be large, well below the threshold for the parent ion, since absorption is still occurring. The fact that the threshold for the hydrate is near 1.67 eV rather than the 1.52 eV expected for the origin of the CO_3^- excited state could be due to a slight perturbation of the excited state due to hydration. The magnitude of the perturbation, a gas phase "solvent shift" of 0.15 eV, is comparable to that for O_3^-, and the direction of the shift is the same.

IV O_4^- PHOTODESTRUCTION

Figure 2 shows the extension of previous O_4^- photodestruction cross section measurements[5] to lower energies. An apparent photodestruction threshold of 7900 Å is indicated by the linear decrease of the cross section and the low values measured at longer wavelengths. The smooth, structureless decline in this cross section above 6000 Å is similar to that observed for positive ion molecular dimers[10,16] such as $NO \cdot NO^+$ and O_4^+, and may indicate

similarities in bonding and structure. A pseudodiatomic model for these dimer ions would suggest a bound state with the charge shared equally between fragments. In analogy with the diatomic rare gas ions,[16] this state would be coupled by an optical transition to a repulsive excited state. In addition to the photodissociation, photodetachment of O_4^- is also thermodynamically allowed at the present wavelengths. The presence of large amounts of photodetaching O_2^- in the ion swarm, however, prevented experimental determination of the photodestruction channels.

The small positive cross sections ($\sim 1 \times 10^{-19}$ cm^2) at wavelengths longer than 7600 Å are difficult to interpret. An equilibrium[17]

$$O_2^- + 2O_2 \rightleftarrows O_4^- + O_2 \quad k_f = 4 \times 10^{-31} \text{ cm}^6/\text{s}$$
$$k_r = 2.7 \times 10^{-14} \text{ cm}^3/\text{s} \qquad (4)$$

exists which interconverts a fraction of the O_2^- and O_4^- ions while they traverse the laser interaction region. This can result[10a] in an apparent decrease in the O_4^- signal when the laser is on due to photodetachment of precursor O_2^-. Application of the kinetic model of reference 10a to this system predicts an apparent O_4^- photodestruction cross section of only $\sim 2 \times 10^{-20}$ cm^2 from this effect. An additional source of subthreshold photodestruction would be the presence of vibrationally excited O_4^- ions in the laser interaction region. At the drift tube conditions of this experiment, 1.5% of the O_4^- ions detected by the quadrupole mass spectrometer will have been formed by reaction (4) in the laser interaction region, and are subject to laser photodestruction prior to thermalizing collisions. The exothermicity of reaction (4) is 0.6 eV,[18] and a significant fraction of

this energy likely appears as internal excitation of the nascent O_4^- ions. If these excited ions have large photodestruction cross sections ($\sim 10^{-17}$ cm^2), the observed photodestruction at wavelengths longer than 7600 Å might be attributed to excited O_4^-. Thus, the threshold for photodestruction of ground state O_4^- ions could be as high as 1.63 eV.

V PHOTODESTRUCTION CROSS SECTIONS FOR OTHER SPECIES

Table II lists upper limits for the photodestruction cross sections of a number of negative ions of atmospheric interest derived from measurements at 8250 Å (1.50 eV), 7500 Å (1.64 eV), 7100 Å (1.74 eV) and/or 6800 Å (1.82 eV). All upper limits quoted in Table II represent the largest possible photodestruction cross section of the species within one standard deviation statistical error of the measured values. Cross sections of zero are included within the precision of all these measurements. Although measurements were not made for some ions at the longest wavelengths, cross sections of less than 1×10^{-19} cm^2 are indicated by extrapolation. The thermodynamic threshold for NO_2^- detachment[11,19] lies at shorter wavelengths, so NO_2^- was not investigated. $NO_3^- \cdot H_2O$ could not be examined since the $O_2^- \cdot NO \cdot H_2O$ isomer was preferentially produced under our experimental conditions.[6]

Except for O_4^- and $CO_3^- \cdot H_2O$ which are photodissociated below 7600 Å, and the less precise 8250 Å measurement for $CO_4^- \cdot H_2O$, which can be formed only in small quantities in the drift tube, the results indicate cross sections less than 1×10^{-19} cm^2 for all of these ions over the wavelength range studied. The measurements are consistent with, and imply, cross sections of zero. Many of these ions are characterized[14] as weak, electro-

statically bound cluster ions, and have low thermodynamic thresholds for dissociation. Yet, no repulsive or predissociative states that lead to photodissociation appear to exist below 1.6 eV. The photodetachment threshold for these ions is also apparently at shorter wavelengths. Since the neutral clusters are not bound (except for a few meV from weak van der Waals forces), the necessarily dissociative photodetachment will require higher photon energy than photodissociation of the parent ion. The results also confirm that the O_3^-, CO_3^-, $O_2^- \cdot NO$, and CO_4^- thresholds measured previously[5,6] are true thresholds. We thus conclude that none of the atmospheric negative ions studied is likely to have significant photodestruction cross sections in the infrared region of the solar spectrum.

This work helps locate the threshold for $O_2^- \cdot H_2O$ photodestruction. Previous measurements[5] indicate the cross section is less than 2×10^{-19} cm^2 at 6700 Å. Current measurements give a value less than 1.0×10^{-19} cm^2 at 7200 Å, indicating a threshold of 1.8 ± 0.1 eV (6900 Å). Accurate measurements at intermediate wavelengths have not been attempted because of the small $O_2^- \cdot H_2O$ ion current, the small cross sections, and the possible coupling[10] of O_2^- and O_4^- photodestruction into the measured $O_2^- \cdot H_2O$ value via the reactions:

$$O_2^- + H_2O + O_2 \rightleftarrows O_2^- H_2O + O_2 \qquad (5)$$

and

$$O_4^- + H_2O \rightleftarrows O_2^- H_2O + O_2 \ . \qquad (6)$$

VI CONCLUSIONS

Upper limits of 1×10^{-19} cm^2 have been established for the photodestruction cross sections of many negative ions of atmospheric interest for photon energies less than 1.6 eV. Few of these ions undergo photodestruction below 1.8 eV. Thresholds for $CO_3^- \cdot H_2O$, O_4^-, and $O_2^- \cdot H_2O$ were established. Except for O_2^-, no infrared photodestruction of D-region negative ions appears important. Table III summarizes photodestruction cross section values for these ions measured in this and previous studies.[3-8]

ACKNOWLEDGEMENTS

The authors gratefully acknowledge the use of a laboratory computer system purchased through an equipment grant from the National Science Foundation.

REFERENCES

*This work was supported by the U.S. Army Ballistics Research Laboratories through the U.S. Army Research Office.

1. L. Thomas, Radio Sci. 9, 121 (1974); F. E. Niles and M. G. Heaps, Abstract J163, IAGA/IAMAP Joint Assembly, Seattle, 1977.

2. W. L. Nighan and W. J. Wiegan, Phys. Rev. A10, 922 (1974).

3. J. T. Moseley, P. C. Cosby, R. H. Bennett, and J. R. Peterson, J. Chem. Phys. 62, 4826 (1975).

4. P. C. Cosby, R. A. Bennett, J. R. Peterson, and J. T. Moseley, J. Chem. Phys. 63, 1612 (1975).

5. P. C. Cosby, J. H. Ling, J. R. Peterson, and J. T. Moseley, J. Chem. Phys. 65, 5267 (1976).

6. J. T. Moseley, G. P. Smith, J. R. Peterson, and P. C. Cosby, to be submitted for publication; J. T. Moseley, P. C. Cosby, J. R. Peterson, and G. P. Smith, Abstract MA-7, 30th G.E.C., Bull. Am. Phys. Soc., in press, (1977).

7. P. C. Cosby, J. T. Moseley, and G. P. Smith, submitted to J. Chem. Phys.; P. C. Cosby, G. P. Smith, J. H. Ling, J. R. Peterson, and J. T. Moseley, X ICPEAC Abstracts, Paris, 1977, p. 111.

8. J. T. Moseley, L. C. Lee and G. P. Smith, in preparation.

9. Laser dyes: Oxazine 1 Perchlorate (Eastman 11885, New England Nuclear Pilot 740); DEOTC (Eastman 14354); DEOTC Perchlorate (Nippon KanKoh-Shikiso Kenkyusho (NK-2420); and Rhodamine 640 Perchlorate (Exciton Chemical Co.).

10. G. P. Smith, P. C. Cosby, and J. T. Moseley, J. Chem. Phys. 67, 0000 (1977); J. A. Vanderhoff, J. Chem. Phys. 67, 2332 (1977).

11. B. A. Huber, P. C. Cosby, J. R. Peterson, and J. T. Moseley, J. Chem. Phys. 66, 4520 (1977).

12. L. M. Branscomb, S. J. Smith, and G. Tisone, J. Chem. Phys. 43, 2906, (1965).

13. H. W. Ellis, R. Y. Pai, E. W. McDaniel, E. A. Mason, and L. A. Viehland, At. Data Nucl. Data Tables 17, 177 (1976).

14. F. C. Fehsenfeld and E. E. Ferguson, J. Chem. Phys. 61, 318 (1974).

15. J. T. Moseley, P. C. Cosby, and J. R. Peterson, J. Chem. Phys. 65, 2512 (1976).

16. L. C. Lee, G. P. Smith, T. M. Miller, and P. C. Cosby, submitted for publication; L. C. Lee, G. P. Smith, T. M. Miller, and P. C. Cosby, Abstract BA-5, 30th G.E.C., (1977), Bull. Am. Phys. Soc., to be published.

17. J. L. Pack and A. V. Phelps, Bull. Am. Phys. Soc. 16, 214 (1971).

18. D. C. Conway and L. E. Nesbitt, J. Chem. Phys. 48, 509 (1968).

19. E. Herbst, T. A. Patterson, and W. C. Lineberger, J. Chem. Phys. 61, 1300 (1974).

Table I

EXPERIMENTAL CONDITIONS

Ions	Gas	P (torr)	Mobility ($cm^2/V\ s$)[3-5,13]
O_3^-	O_2	0.5	2.54
O_4^-	O_2	0.5	2.16
$O_2^- \cdot H_2O$	O_2/trace H_2O	0.5	2.5
$O_3^- \cdot H_2O$	O_2/trace H_2O	0.6	2.2
CO_3^-	7% CO_2 in O_2	0.2	2.4
$CO_3^- \cdot H_2O$	7% CO_2 in O_2/trace H_2O	0.5	2.3
CO_4^-	7% CO_2 in O_2	0.2	2.3
$CO_4^- \cdot H_2O$	7% CO_2 in O_2/trace H_2O	0.5	2.2
HCO_3^-	2% CH_4 in CO_2	0.5	1.34
$HCO_3^- \cdot H_2O$	2% CH_4 in CO_2/trace H_2O	0.5	1.34
NO_3^-	2% NO in O_2	0.6	2.2
$NO_2^- \cdot H_2O$	2% NO in CO_2/trace H_2O	0.5	1.5
$O_2^- \cdot NO$	N_2O/trace O_2	0.5	1.6
$O_2^- \cdot NO \cdot H_2O$	N_2O/trace H_2O,O_2	0.5	1.5

Table II

UPPER LIMITS ON PHOTODESTRUCTION CROSS SECTIONS

(10^{-18} cm^2)

λ (Å)	8250	7500	7100	6800
E (eV)	1.50	1.64	1.74	1.82
CO_3^-	< 0.088	< 0.065	< 0.080	
$CO_3^- \cdot H_2O$	< 0.085	< 0.30	(1.7 ± .2)*	
CO_4^-	< 0.115	< 0.020		
$CO_4^- \cdot H_2O$	< 0.192	< 0.064		
HCO_3^-	< 0.052	< 0.044	< 0.022	
$HCO_3^- \cdot H_2O$	< 0.038	< 0.073	< 0.025	
O_4^-	< 0.058	(0.32 ± .05)	(0.46 ± .05)	
$O_2^- \cdot H_2O$	< 0.093	< 0.12	< 0.10	
O_3^-				< 0.089
$O_3^- \cdot N_2O$				< 0.023
$O_2^- \cdot NO$	< 0.087		< 0.054	
$O_2^- \cdot NO \cdot H_2O$	< 0.072	< 0.036		
NO_3^-				< 0.082
$NO_2^- \cdot H_2O$			< 0.041	

*Values in parentheses are measured values, not upper limits.

Table III

PHOTODESTRUCTION CROSS SECTIONS OF ATMOSPHERIC NEGATIVE IONS (10^{-18} cm^2)

ION	Photon Energy (eV)													Products
	1.5	1.6	1.7	1.8	1.9	2.0	2.1	2.2	2.3	2.4	2.5	2.6	2.7	
CO_3^-	< .09	< .07	< .04	0.2	2.0	1.5	1.5	1.5	1.2	0.8	0.4	0.6	0.9	$O^- + CO_2$
$CO_3^- \cdot H_2O$	< .09	< .10	.55	7.5	7.5	7.5	7.5	7.0	5.5	3.5	2.5	2.0	2.0	$CO_3^- + H_2O$
CO_4^-	< .12	< .02	< .02	< .03	< .02	< .02	< .03	< .02	< .02	.04				b
$CO_4^- \cdot H_2O$	< .19	< .06	(0)[c]	(0)	(0)	(0)	(0)	(0)	(0)	< .07				
HCO_3^-	< .05	< .04	< .02	< .02	< .03	< .03	< .03	< .03	< .03	< .02	< .03	< .04	< .05	
$HCO_3^- \cdot H_2O$	< .04	< .07	< .03	(0)	(0)	(0)	(0)	(0)	(0)	< .01	(0)	(0)	(0)	
O_2^-	0.8	0.9	1.0	1.1	1.2	1.3	1.4	1.5	1.6	1.7	1.8	2.0	1.8	$e^- + O_2$
$O_2^- \cdot H_2O$	< .09	< .12	< .10	.12	.15	0.3	0.4	0.5	0.5	0.5				b
O_3^-	(0)	(0)	(0)	< .09	.02	.05	0.3	0.92	2.15	3.82	5.0	6.0	5.0	$O^- + O_2$
$O_3^- \cdot H_2O$	(0)	(0)	(0)	< .02	< .02	.03	0.1	0.56	1.64	3.28				$O_3^- + H_2O$
$O_3^- \cdot 2H_2O$	(0)	(0)	(0)	(0)	(0)	.02	.08	0.37	1.1	2.3				
O_4^-	< .06	.22	.35	.65	.75	1.1	1.2	1.4	1.3	1.7	1.7	2.1	1.9	b
NO_2^-	(0)	(0)	(0)	(0)	< .01	(0)	(0)	(0)	(0)	< .06				$e^- + NO_2$
$NO_2^- \cdot H_2O$	(0)	(0)	< .04	(0)	(0)	(0)	(0)	(0)	(0)	< .02	(0)	(0)	(0)	
NO_3^-	(0)	(0)	(0)	< .08	(0)	< .01	(0)	(0)	(0)	< .01	(0)	(0)	(0)	$e^- + NO_3$
$O_2^- \cdot NO$	< .09	< .09	< .05	< .05	.04	.09	.19	.34	.73	1.3				$O_2^- + NO$
$O_2^- \cdot NO \cdot H_2O$	< .07	< .04	< .04	(0)	(0)	.01	.03	.08	.16	.53				

a) Ar^+ laser lines

b) Photodetachment may occur

c) Zero values in parentheses are indicated by energetics, extrapolation or behavior of the parent ion.

FIGURE CAPTIONS

1. Photodissociation cross sections for CO_3^- and $CO_3^- \cdot H_2O$ vs. photon energy and wavelength. Data points for $CO_3^- \cdot H_2O$ above 6950 Å are from this work; the other data is from Ref. 3.
2. Photodestruction cross sections for O_4^-. Data above 6950 Å this work; data below 6950 Å is from Ref. 3.

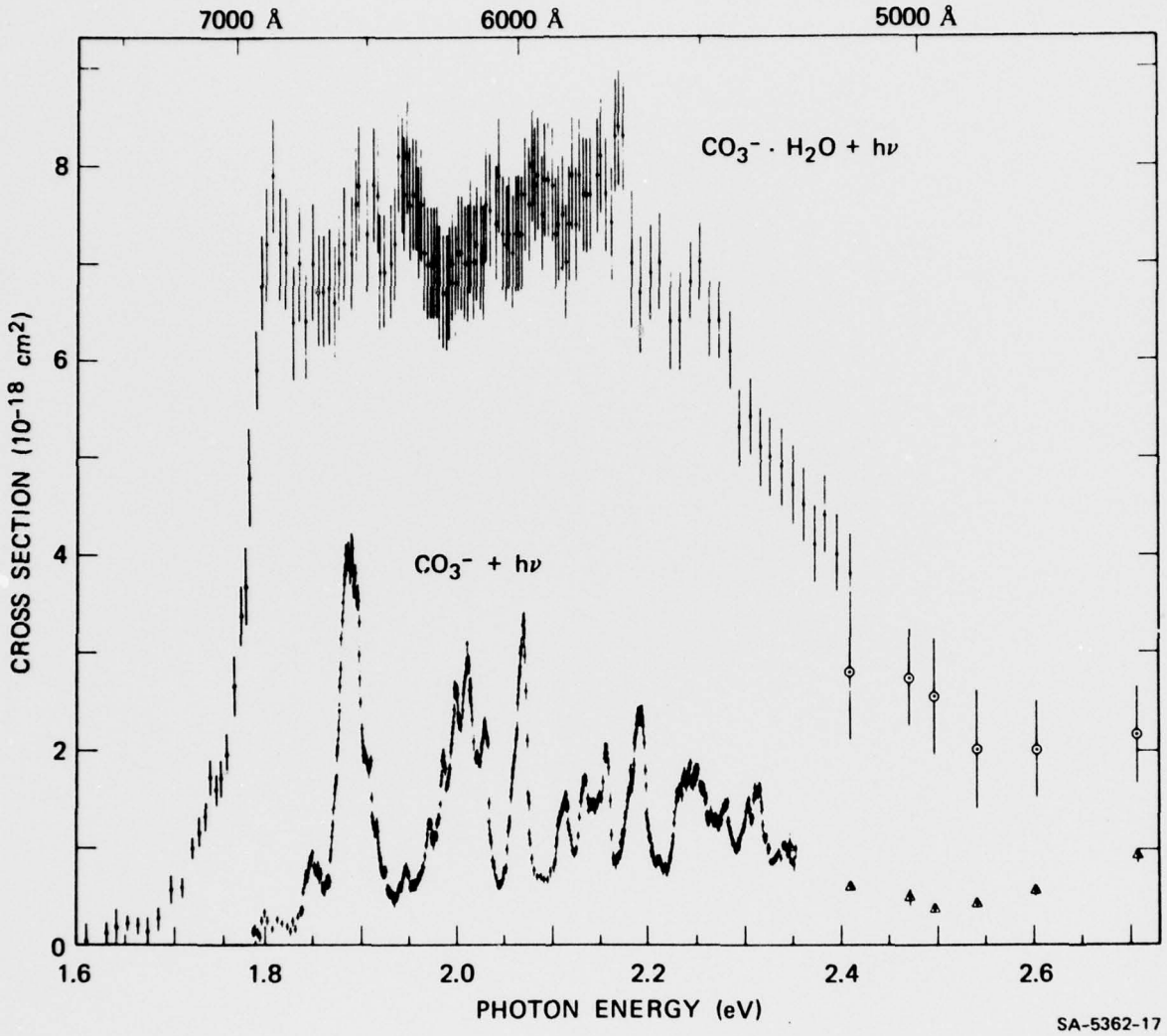
7000 Å
6000 Å
5000 Å
$CO_3^- \cdot H_2O + h\nu$
$CO_3^- + h\nu$
CROSS SECTION (10^{-18} cm^2)
0
2
4
6
8
1.6
1.8
2.0
2.2
2.4
2.6
PHOTON ENERGY (eV)
SA-5362-17

Figure 1

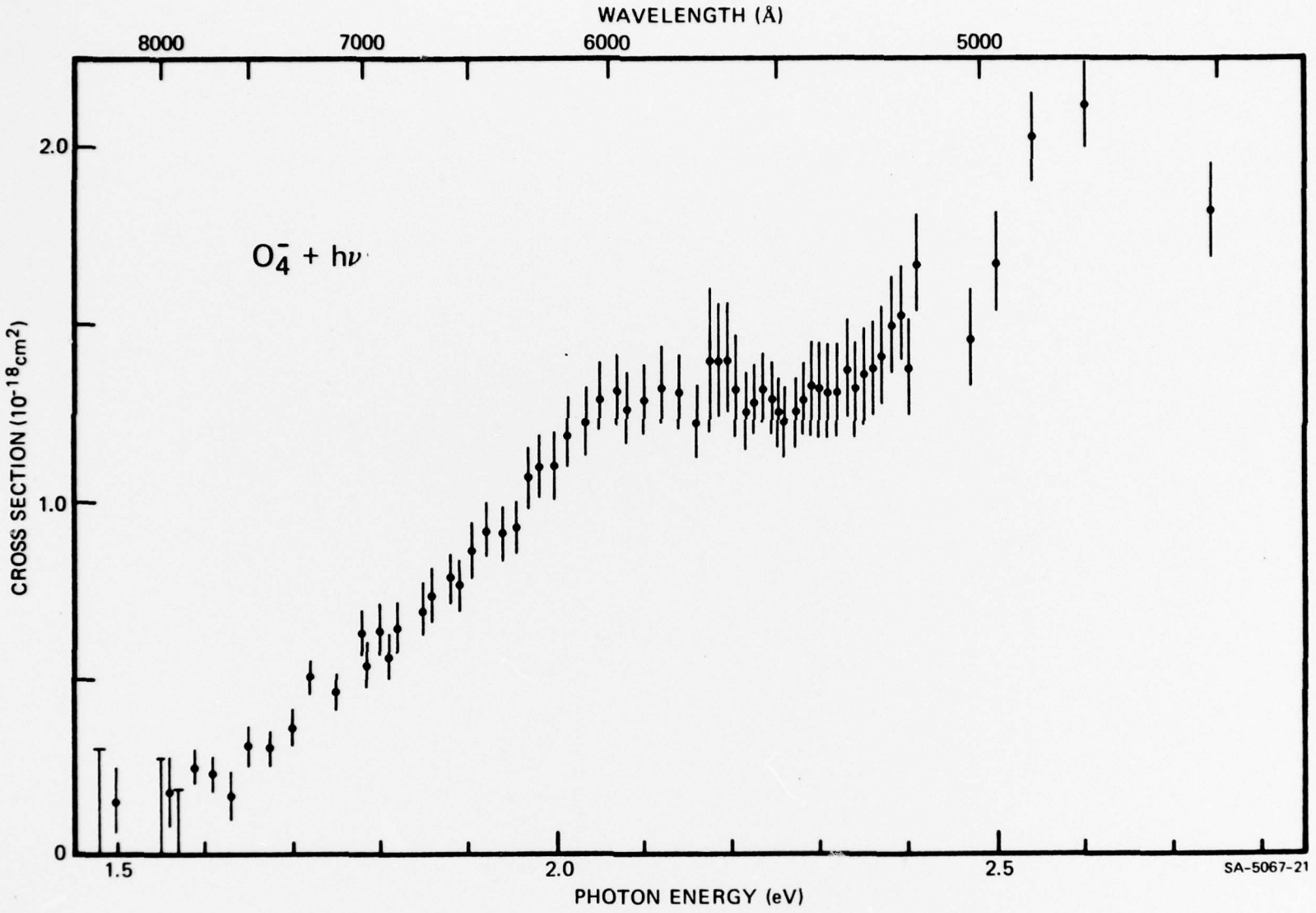
WAVELENGTH (Å)
8000
7000
6000
5000
2.0
1.0
0
$O_4^- + h\nu$
CROSS SECTION (10^{-18} cm^2)
1.5
2.0
2.5
PHOTON ENERGY (eV)
SA-5067-21

Figure 2